University of Alberta

Dengue NS1 Detection using Chemically Modified Silicon Micropillars

by

Minashree Singh

A thesis submitted to the Faculty of Graduate Studies and Research in partial fulfillment of the requirements for the degree of

Master of Science

in

Pharmaceutical Sciences

Faculty of Pharmacy and Pharmaceutical Sciences

Fall 2012
Edmonton, Alberta

To my Parents, my Family and Soul-mate

Abstract

Dengue fever is a mosquito born viral disease that is reaching epidemic proportions. Despite of various control means, it is still flourishing and is becoming a major health concern around the world. In this thesis, a novel diagnosis method for the detection of Dengue virus has been developed. Micro-spot-integrated pillars chip (MSIP) has been used to increase the surface area for the immunoreaction and hence the probability of the Dengue virus detection. The MSIP chip used for the diagnosis of Dengue NS1 was chemically modified to immobilize the capture antibodies. Each step of the surface modification and biofunctionalization process was characterized by using different characterization tools. An automated and unsupervised algorithm was developed to quantify the fluorescent signal. The result showed that the method developed was five fold more sensitive than the immunoassay performed on chemically modified at silicon substrate and hence, meet the objective of the thesis.

Acknowledgements

First and foremost, I would like to thanks my supervisor Dr. Kamaljit Kaur and co-supervisor Dr. Sushanta Mitra, who has taught me research- how to conduct, proceed, think, persevere and present; enlighted me all throughout my masters degree with there suggestions and knowledge. I am indebted to MNTL research group; Naga Siva Kumar Gunda, Jerry Joseph, Prashant Waghmare, Siddhartha Das, Dibyo Sarkar and Anil Stephen. Naga Siva Kumar Gunda deserves special thanks for his guidance, support and advice, which helped me through my journey of developing the project and writing the thesis. He has subtly instilled in me some invaluable attributes that I am sure, I will carry lifelong.

The work would not have completed without the generous support and technical advice of Ni Yang and Lana Norman. Their help and guidance while characterizing the samples was very crucial to the project. I am also indebted to Advaitya Ganguly for providing me the antibodies for my research work.

I would like to thank Dr. Lavasanifer, who was in my supervisory committee for her valuable suggestions and advices that went a long way in improving my thesis.

I would also like to acknowledge Dr. Suresh for providing me the financial support throughout my masters. The fund was provided from Dr. Suresh general fund from Faculty of Pharmacy and Pharmaceutical Sciences.

The indirect support and encouragement of my friends; Vivek, Yash, Shishir, Chaitaniy, Shiv, Manjeet, Nagi, Anirban, Stella and Ganesh has helped me stay focused and motivated. Veena, Sampada and Rajesh made my university life easy. I am also grateful to my family (Bhaiya and Didis) for loving me and supporting me in each walk of my life. Lastly, and most importantly, I want to thanks my parents for bringing me to this world, raising me, supporting me, and being my first teachers. I would not have achieved anything without their selfless, benign love and wishes.

Table of Contents

[1] An adaptation of this chapter has been submitted to *Surface Science*, September 2012, *In Review*

[2] An adaptation of this chapter has been submitted to *Lab on a Chip*, September 2012, *In review*

[3]This appendix has been included as supplementary material for chapter 3 which is submitted for publication in *Lab Chip*, September 2012, *In review*

List of Tables

List of Figures

Nomenclature

Abbreviations

AFM Atomic Force Microscopy

AFP Alfa Feto Protein

APS Amino-propyl silane

APTES (3-Aminopropyl)-triethoxysilane

C Capsid protein

CA Contact angle measurement

CF Complement fixation

DF Dengue Fever

DHF Dengue Hemorrhagic Fever

DPF Discrete probability function

DSS Dengue Shock Syndrome

E Envelop glycoprotein

EDC Ethyl- (dimethyl)-aminopropyl carbodiimide

ELIS Enzyme-linked immunosorbent assay

FITC Fluorescein isothiocyanate

FM Fluorescence microscopy

FTIR Fourier transforms infrared spectroscopy

HI Hemagglutination-inhibition

HIgG Human Immunoglobulin G

MSIP Micro-spot integrated pillar chip

NHS N-Hydroxysuccinimide

NSq Square arrangement

NSt Staggered arrangement

NT Neutralization test

PBS Phosphate buffer solution

PKMC Probabilistic k-means clustering

PPR Positive photoresist

prM Membrane protein

RMS Root-mean-square

RNA Ribonucleic acid

RT-PCR Reverse transcriptase Polymerase Chain Reaction

SAM Self assembled monolayer

SEM Scanning electron microscopy

WHO World Health Organization

Chapter 1

Introduction

Mosquitoes are potent agents in carrying viruses, parasites and transmitting them from one individual to another. These viruses and parasites can cause life-threatening diseases in humans. It has been estimated that they transmit diseases to more than 700 million people annually and, with many of them resulting in deaths [1]. Despite of various control efforts mosquito borne diseases are still flourishing and are a major health concern around the world. Malaria, for example, continues to be a major factor of deaths especially amongst children and infants. Around 40 % of world's population is vulnerable to malaria and it is reported to be responsible for approximately one million deaths and 300 - 500 million cases of infection [2–5]. Yellow fever is another example of viral fever transmitted by the bite of mosquitos, which takes a death toll of 30,000 annually [6]. Dengue is another kind of deadly mosquito borne viral disease that can quickly reach epidemic proportions and is the main topic of research in this work.

1.1 Dengue as global health problem

The first records of Dengue as a fever dates as far back as 992 A.D. in China, although as an epidemic it first occurred in 1779-1780 [8–10] with simultaneous outbreaks in Asia, Africa and North America. The occurrence of dengue as an epidemic was not so frequent until the second world war but during and post world war II, the infection spread very fast, as high as 30 times, from 1960

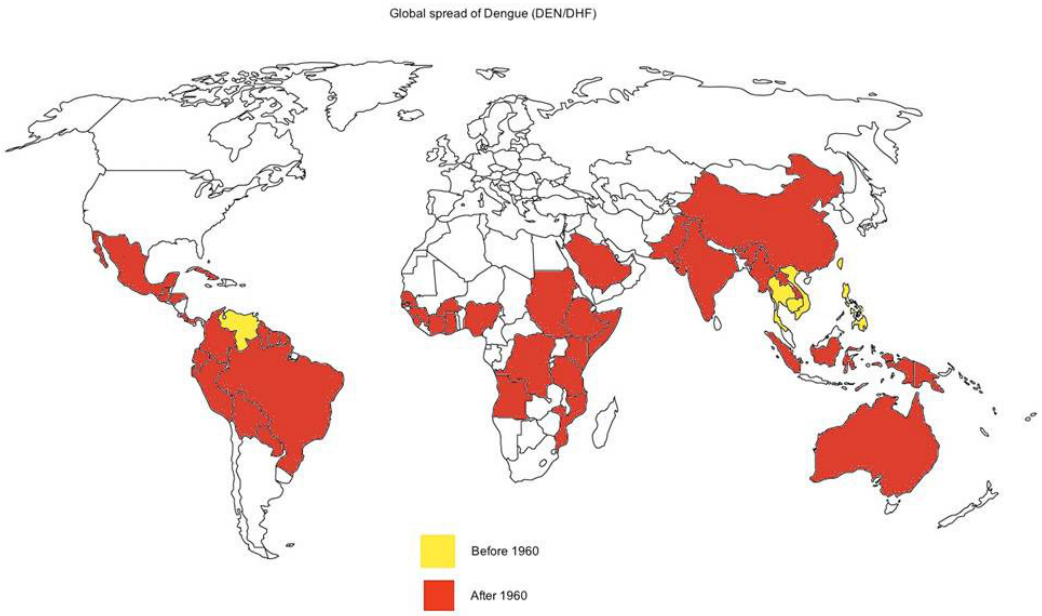

Figure 1.1 – Countries affected with Dengue fever and Dengue Hemorrhagic before and after 1960(Adopted from WHO report [7]).

to 2010. Currently about 2.5 billion people, or 40% of the world's population are susceptible to dengue infection and it is reported that 50 to 100 million infections occur annually, including 500,000 Dengue Hemorrhagic Fever(DHF) cases and 22,000 deaths [11, 12]. Fig. 1.1 shows the countries affected with Dengue fever and Dengue Hemorrhagic before and after 1960.

1.1.1 Reasons for emergence of Dengue

Several reasons have been associated with the emergence of dengue. Some of the them are; lack of effective mosquito control measures in dengue affected countries, sudden and uncontrolled growth of urban population leading to inadequate public health care systems such as sewage and waste management, increase in international travel via airplanes, lack of public awareness about the disease and its prognosis measures and ecological changes such as global warming [13–15].

1.2 Dengue virus

Dengue fever is caused by dengue virus, which is a single stranded positive RNA virus from the family *Flaviviridae* of genus *Flavivirus*. As known the genomic RNA is responsible for causing infection and producing virions in the host cell. The dengue virus genome contains 11,000 nucleotide base [16], which codes for ten different type of proteins; three of which are structural proteins; Capsid protein (C), Membrane protein (prM), Envelop glycoprotein (E); seven of them are non-structural proteins, NS1, NS2a, NS2b, NS3, NS4a, NS4b, NS5; short non-coding regions on both the 5' and 3' ends. The structural protein forms the coat of the virus and helps in delivering the RNA to the target host cell. The non-structural proteins organizes the production of new virus in the host cell. The virus is enclosed within a lipid membrane that serves as an envelope and 180 identical copies of the envelope protein are attached to the surface of the membrane by a short transmembrane segment [16]. The envelope proteins help in attaching the virus to the host cell surface and begin the process of infection. Fig. 1.2 shows the dengue viral genome structure showing the structural and non-structural proteins present in the dengue virus.

There are four antigenically different serotypes of the virus; DENV1, DENV2, DENV3 and DENV4 base pairs. The four dengue virus serotype differs in nucleotide sequence by 25-35 basepairs [16]. Out of these four different serotypes, DENV4 appears to be most divergent followed by DENV2. DENV1 and DENV3 are more closely related.

1.2.1 Dengue virus life cycle

Dengue virus can follow two types of cell cycle depending upon the type of strain; sylvatic and epidemic cycle [18, 19]. Fig. 1.3 shows the two types of life cycle followed by dengue virus. The sylvatic transmission cycle involves transmission between nonhuman primates and forest dwelling *Aedes aegypti*. Infection in humans by sylvatic cycle is rare. Whereas the endemic or epidemic cycle involves transmission between either humans and *A. aegypti* or humans

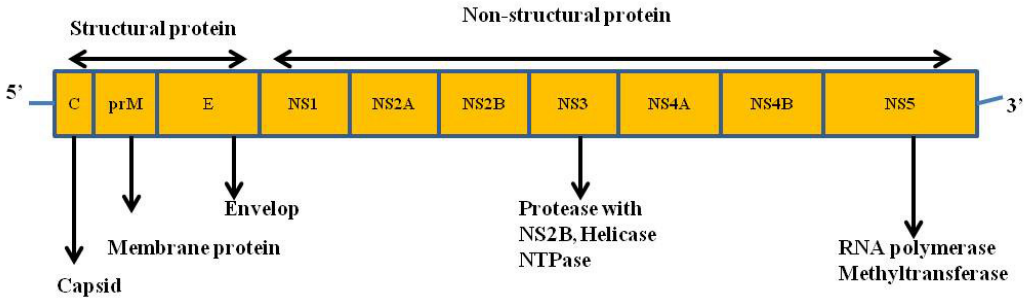

Figure 1.2 – The Dengue viral genome structure showing gene order. Structural proteins: C, capsid; E, envelope and prM, premembrane. NS and nonstructural proteins (Adopted from Whitehead et al. [17]).

and *A. albopictus*. Sometimes other mosquitoes acts as secondary vectors. Endemic dengue is most common in tropical urban slums where poor sanitation and the stagnant water has allowed the number of mosquito vectors to rise. An increase in global population and number of mosquitoes in urban regions has lead to manifold rise in dengue virus transmissions.

1.2.2 Dengue transmission in humans

Dengue viruses are transmitted to humans through the bite of female *Aedes aegypti* or *Aedes albopictus* mosquitoes. Furthermore, the mosquitoes themselves acquire these viruses by feeding on infected human blood. Once infected, it takes eight to ten days for the virus incubation and then the infected mosquito becomes capable of transmitting the virus to humans. This process continues through its entire life and the virus may get transmitted to next generation by means of transovarial transmission (via the eggs). Humans serve as the main multiplying platform for the virus and act as a source of virus for the uninfected humans. The virus circulates in humans for about 2-7 days. Aedes mosquito would acquire the virus while feeding on the human blood during this time. In some places of the world, the transmission cycle may involve human primates.

In general, dengue virus transmission has two patterns namely epidemic

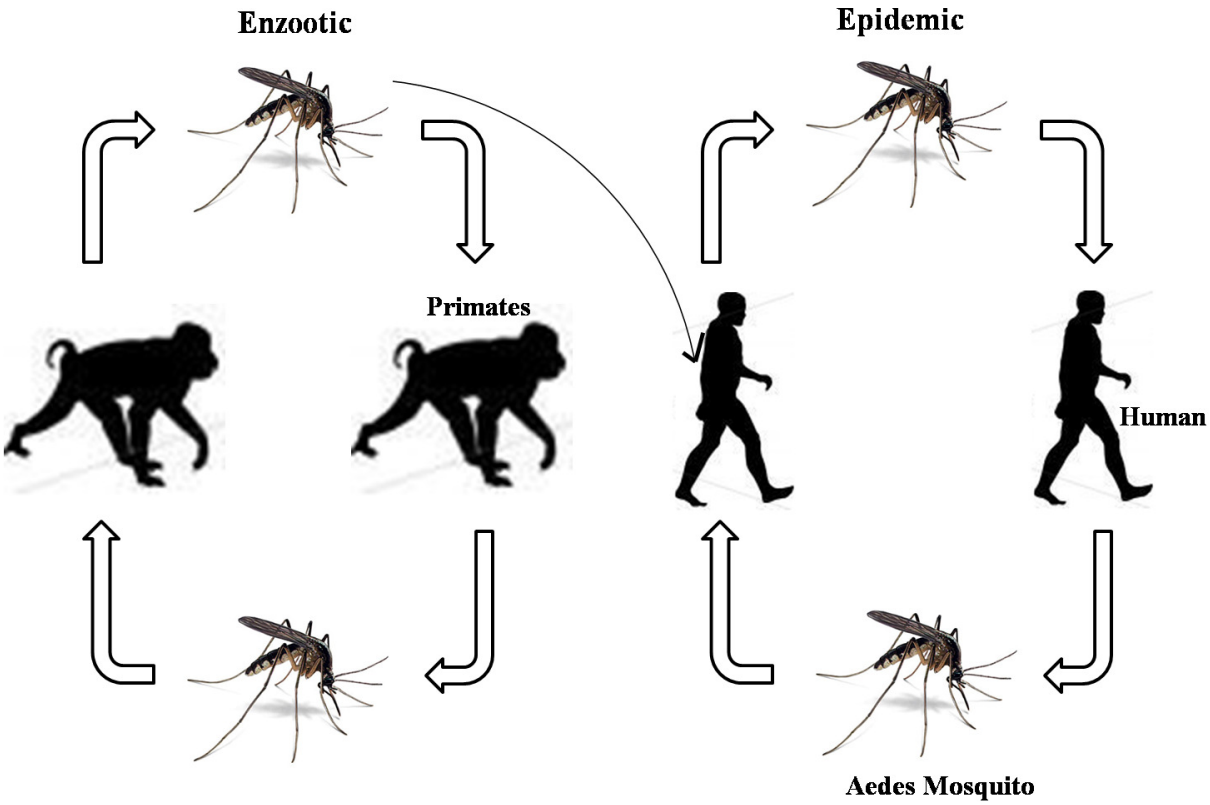

Figure 1.3 – The Sylvatic and Endemic Dengue Transmissions Cycles (Adopted from Whitehead et al. [17]).

dengue and hyperendemic dengue. Epidemic dengue transmission occurs when only one viral strain is involved and the virus is introduced into a isolated region while the hyperendemic dengue transmission occurs when multiple strains are involved and there is a continuous circulation of multiple viral stereotype.

1.3 Dengue Fever: Clinical Diagnosis

Dengue disease can be classified into four types as shown in Figure 1.4 [20] .

1.3.1 Non-specific febrile illness

It is characterized by occurrence of maculo-popular rash, mostly in children and upper respiratory features are also commonly observed, especially pharyngitis [21].

1.3.2 Classical Dengue Fever (DF)

A wide array of symptoms of dengue can be observed depending upon the case and the patient, although the onset is usually characterized by fever. Different types of aches and pains may occur such as severe headache, retro-orbital pain, fatigue, loss of appetite, nausea, vomiting and abdominal pain. Myalgias and arthralgias (severe pain in legs and joints also called break-bone fever or bone crusher disease) also are common symptoms during first hours of illness. The fever may last from 3-7 days and shows a biphasic pattern with a smaller peak of fever towards the trailing end of the disease [14, 21–24].

1.3.3 Dengue Haemorrhagic Fever (DHF)

Approximately 1 of 100 dengue fever takes the form of dengue haemorrhagic fever in later stages and is characterized by increased vascular permeability, hypervolemia and abnormal blood clotting mechanisms [20]. The symptoms of DHF are similar to those of DF along with at least one of the following [14]: Pain in abdomen, bleeding from the nose, mouth and gums or skin bruising, vomiting sometimes accompanied with blood, black stools like coal tar, thrust,

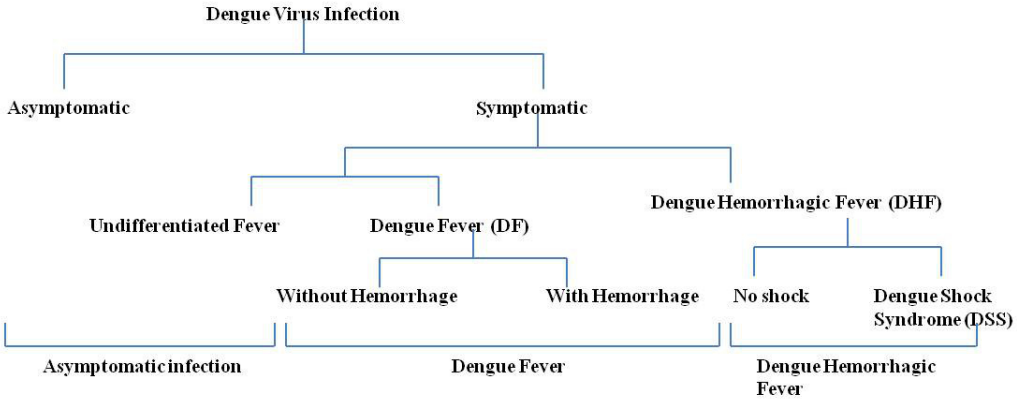

Figure 1.4 – Clinical representation of manifestation Dengue infection (Adopted from Coffey et al. [25]).

sweating and cold extremities, restlessness, or sleepiness. The fever last for about 2-7 days and most patients recover but in severe cases patients may show indications of circulatory failures [23].

1.3.4 Dengue Shock Syndrome (DSS)

DSS is probably the most fatal of all dengue fevers and has a mortality rate of 44 [26]. Symptoms of DSS are similar to those of DHF plus narrow blood pressure or hypotension and decrease in platelet count [20]. Patients succumb to death because of multi-organ failure and disseminated intra vascular coagulation [20].

1.4 Diagnostic Techniques

1.4.1 Dengue Diagnosis and Laboratory Tests

An early and accurate diagnostic test is vital for rapid detection, confirmation of acute condition, surveillance activities and epidemic outbreak control. Laboratory diagnosis of dengue virus can either involve detection of viral antigens or specific antibodies in the patient's serum [26–28]. Virus isolation, nucleic acid or antigen detection techniques are commonly used for early stages of detection while serology may be used at the end of the acute phase [20]. A

wide range of diagnostic techniques exists for dengue prognosis but the choice of diagnostic method largely depends on the purpose for which the test is conducted, type of facilities and expertise available and cost and time involved [20]. The purpose could be clinical trials, surveillance and outbreak investigations, and vaccine development. Table 1.1 shows proposed product specifications for various purposes [29]. Generally tests with high efficiency and accuracy require more complex procedures and technical expertise for example virus isolation and nucleic acid detection involves greater man-hours and are tedious. Serology, on the other hand, is more indirect and may compromise sensitivity and specificity to gain ease of performance [20].

Table 1.1 – Characteristics of diagnostics tests based on purpose of use.

Purpose	**Diagnostic Test**
Early diagnosis	- Distinguishes between dengue and other diseases with similar clinical presentations - Highly sensitive during the acute stage of infection - Provides rapid results - Inexpensive and easy to use - Stable at temperatures greater than 30^0 for field use, if necessary
Epidemiological surveillance and outbreak investigations	- Positive as soon as possible after onset of symptoms to provide early warning - Highly specific - Determines dengue virus serotype - Distinguishes between primary and secondary infection - High throughput capacity - Long shelf life
Vaccine efficacy trials	- Provides virological diagnosis of dengue virus infection during the febrile phase - Distinguishes between dengue and other flaviviruses - Distinguishes between dengue serotypes - Distinguishes between first and subsequent infections - Provides a marker severe disease easy to use

1.4.2 Current Dengue Diagnostic Methods

Virus Isolation

There are four popular techniques to isolate the dengue virus: 1) intracerebral inoculation of 1- to 3-day-old baby mice, 2) the use of mammalian cell cultures (primarily LLC-MK2 cells), 3) intrathoracic inoculation of adult mosquitoes, 4) the use of mosquito cell cultures [26–28].

Baby mice method can be used to isolate all 4 types of dengue sterotypes [30] but the process is very time consuming and expensive. As it has low sensitivity, wild-types viruses cannot be isolated. One of the advantages of using the baby mice method is that it helps to isolate other arboviruses that cause dengue-like illness. Mammalian cell culture technique also suffers from the same kinds of disadvantages as baby mice method i.e. it is slow, expensive and less sensitive [26, 27].

Mosquito inoculation is the most sensitive amongst all the 4 virus isolation methods [26, 31] with isolation rates of up to 100 of serologically confirmed dengue infections. It is also most commonly used for routine successful virologic confirmation of fatal cases [26, 28, 32]. Generally 4 types of mosquitoes are used; A. aegypti, A. albopictus, Toxorhynchities amboinensis, and T. Splenden and both the genders are equally susceptible [14]. Depending upon the incubation temperature, dengue viruses generally replicate to high titers (106 to 107 MID50) in about 4-5 days [14]. Direct fluorescent-antibody DFA test is performed on mosquito tissues, usually brain or salivary glands to detect virus in mosquito [26, 32, 33]. Some of the criticisms the technique faces is for being labour intensive and requiring an insectary to produce large numbers of mosquitoes for inoculation [14].

In mosquito cell culture, three cell lines of comparable sensitivity are most commonly used [34]. The C6/36 clone of A. albopictus cells forms the first cell line [35]. The cell line method serves as a rapid, sensitive and economical method for dengue virus isolation [14] and can also be used for routine virologic surveillance owing to the ease of processing variety of serum specimens [36].

However, the method is less sensitive than mosquito inoculation.

Nucleic acid detection

Reverse transcriptase PCR (RT-PCR) technique has been deployed for a number of RNA viruses in recent years and in case of dengue RT-PCR provides a rapid serotype-specific diagnosis [14]. The process provides a simple, fast and sensitive way to detect viral RNA in human clinical samples, autopsy tissues, or mosquitoes [37, 38]. When compared to C6/36 cell culture, RT-PCR has similar sensitivity but has an added advantage that the outcome of RT-PCR is not influenced by poor handling, poor storage and the presence of antibody. In general, the technique involves three basic steps: nucleic acid extraction and purification, amplification of the nucleic acid and detection and characterization of the amplified product [20]. The setting up of RT-PCR requires high technical skills. It also requires expensive sample and reagents which overall increases the cost for the diagnosis of the disease.

Serological tests

Hemagglutination-Inhibition (HI): HI is simple and rapid diagnostic technique and is very reliable when the protocol is strictly followed [39]. It takes about 5-6 days for the HI antibody (after being infected by dengue virus) to appear at detectable levels. For primary infections, antibody titers in convalescent-phase serum, specimens are generally below 640 while in secondary and tertiary dengue infections the reciprocal antibody titer rapidly increases 5,120 to 10,240 or more [14, 40]. In practice, a titer of 1,280 in an acute-phase or early convalescent-phase serum sample is indicative of current dengue infection [14]. The method is lacks specificity and hence not very commonly used.

Complement Fixation (CF): CF is based on the theory that active serum complement binds to antibody and antigen complex and this antibody-antigen complex inactivates the serum complement which makes it unavailable for

other Ab-Ag pair [41]. This theory is basis for various diagnostic tests which helps in detecting specific antigen and antibody. Some characteristics of CF antibodies are late appearance than HI, greater specificity in primary infections and persistence over short periods with some exceptions [26]. In case of primary infection, greater specificity of CF test compared to HI becomes evident from the fact, that in the CF test responses are monotypic whereas in HI test responses are broadly heterotypic [14]. Although CF test is not very common because it is difficult to perform and requires highly trained personnel, CF test can be useful for patients with current infections.

Neutralization Test (NT): NT is the most specific and sensitive serological test for dengue viruses [42]. It is the most common form of protocol used to quantify the titre of neutralizing antibody for detection of different analytes such as virus. Neutralizing-antibody titers rise faster than CF antibody but slightly slower than the HI and ELISA antibody titers that persist for at least 48 hours [43]. The NT can be used for identification of dengue virus in primary dengue infections because of relatively monotypic neutralizing-antibody responses in properly timed convalescent-phase serum [26, 28]. Determination of the infecting virus serotype by NT or any other serological test is not reliable for any secondary and tertiary infections [44]. The NT can be used for seroepidemiologic studies because of long persistence time. It is not routinely used in laboratories because of the time, expense and technical complexity involved in the process [14].

MAC-ELISA: MAC-ELISA is most widely used serological test for dengue diagnosis as it is simple, rapid and involves very little sophisticated equipment [45, 46]. In the assay, human IgM antibodies are captured on a microtiter plate using anti-human-IgM antibody and this is followed by the addition of dengue virus specific antigen (DENV1-4) [47]. In primary infections IgM antibody titers are significantly higher than the secondary infections and antibody level of IgM drops below detectable levels in approximately 90 days [14]. One of

the limitation that the technique suffers is the cross reactivity with other circulating flaviviruses when multiple flaviviruses co-circulate in the system [47]. On the other hand one major advantage of this assay technique is that it requires only a single, properly timed blood sample and in terms of specificity, it is similar to HI [14].

IgG ELISA: The IgG-ELISA is used to detect previous dengue infection as it can differentiate between primary and secondary dengue infections [26, 47]. Indicators for primary dengue infections are presence of negative IgG in acute phase and a positive IgG in the convalescent phase whereas the presence of positive IgG in the acute phase and a 4 fold rise in IgG titer in the convalescent phase confirm secondary infection [47]. Some of the demerits of IgG-ELISA are less specificity and broad cross-reactivity among flaviviruses [14].

1.5 Immunoassay

Immunoassay is technique that utilizes the highly specific binding between an antigen or heptane and a homologous antibody to detect or measure the concentration of biologically active compound. Solomon Berson and Rosalyn S Yalow were the pioneers who introduced immunoassay in 1959 [48]. Immunoassay is based on the principle of antibody-antigen immunoreactions.

Antibody: Antibodies (Ab), also known as immunoglobulin (Ig) are gamma globulin proteins, which are formed in response to stimulation by foreign substance. Igs can be classified into five groups: IgA, IgG, IgE, IgD and IgM. IgG has a molecular weight of 150kDa and constitutes 80% of the total serum Igs [48]. IgG is tetrameric in structure and is composed of four polypeptide chains; two identical heavy chains (50kDa) and two light chains (25kDa). The N-terminal domains of the heavy and the light chains is highly variable, while the remaining domains have constant sequences. The variable region is know as V region whereas the constant region is know as C region. Antibodies prevent the pathogens from entering or damaging cells by binding non-covalently to the antigens [48]. They also stimulate removal and destruction of pathogens

by phagocytosis and complement mediated cell lysis respectively.

Antigen: Antigens (Ag) are any foreign substance that stimulates the immune response in the body by producing antibodies in the host organism. Hence, the antigens are also referred as immunogens. The immunogens are responsible for the initiating the process of antibody production. The antigens have small antigenic determinant site on their surface, which are known as epitopes. These epitopes are involved in the interaction with the antibodies. The capability of the antigens to interact with the antibodies is also known as antigenicity. Immunogenicity and antigenicity are the two main characteristic features of an antigen.

1.5.1 Principle of Immunoassay

The formation of the antibody-antigen complex is the basis of the immunoassay reaction. This interaction between the Ab and the Ag depends on the equilibrium or affinity constants (K) which is the ratio between rate of association (ka) and dissociation constant (kd) and is given by the following equation[48].

$K = ka/kd.$

The binding of an antigen having one antigenic determinant site can be represented by the following equation:

$$[Ab] + [Ag] \underset{\text{kd}}{\overset{\text{ka}}{\rightleftharpoons}} [Ab - Ag] \tag{1.1}$$

The value of K generally lies in the range of 10^{-6} to 10^{-9} l/mol. Higher the value of the K better it is preferable for the assay. For clinical or diagnostic purposes, either an Enzyme labeled or radio labeled Ag or Ab is used to detect the concentration of the unknown sample. Usually colorimetric, flurometric or chemiluminescent detection methods are used for the detection of enzyme activity. Both quantitative and qualitative analysis can be done using this principle.

1.5.2 The interaction of the antibody molecule with specific antigen:

Immunoassay is known for its specificity and sensitivity because the antibodies react to specific antigens only. The high specificity of the Ab-Ag reactions can be attributed to some of the following reasons.

Hyper variable sequence of the antibodies forms the antigen binding site The V domain of the polypeptide chain of a antibody consist of hyper-variable regions and less variable framework regions . The hyper-variable regions, denoted as HV1, HV2, and HV3 and the framework regions, designated as FR1, FR2, FR3, and FR4 are present on both VH and VL domains of antibody. Beta sheets which provides the structural support to the domain is formed by the framework region whereas loops which are juxtaposed in the folded domain is formed by the hyper-variable region. Thus, the sequence diversity is localized as well as concentrated in particular region of the antibody molecule [49].

Lock and Key model: The binding site of the antibody is formed by the juxtaposition of the complement determining regions (CDR) of the heavy and light chains. This creates the site where antigens can bind to the antibodies [49]. The shapes of the binding site created by the CDRs are different for different antibodies because of the difference in the amino acid (aa) sequence. Thus, the antibodies binds to those antigens whose surfaces are complementary to each other.

Antibodies binds to epitopes present in the antigens: The combining site of an antibody which is located in the Fab region of the polypeptide chain, recognizes the antigenic determinant site present in the antigens and binds with them [49].

Forces involved in Ab-Ag binding: The binding of an antigen to an antibody takes place by the formation of multiple non-covalent bonds. Forces

such as electrostatic force, hydrogen bond and Van Der Waals forces are involved in the formation of these complexes. Electrostatic interactions occur between charged amino acid side chains. Hydrogen bonds get formed when there is electric dipoles in the molecule. Van Der Waals force is a short-range interaction which gets activated when there is a fluctuation in the electron cloud around the molecule [49].

1.6 Rationale

As discussed in the previous sections, dengue is becoming the most common mosquito-borne viral disease of humans causing major concern around the world. Each year, almost 50 million dengue infections are being reported and 500,000 individuals gets hospitalized with dengue hemorrhagic fever in more than 100 countries [50, 51]. Hence, a rapid and accurate diagnosis can help to curb it at its early stages of infection and can help in reducing the severe cases of dengue infection. Therefore in this research, an effort has been made to develop an inexpensive, rapid and highly sensitive diagnostic method for early diagnosis of dengue virus using silicon micropillars.

Several techniques have been developed to ease the whole diagnostic process and to sensitize the immunoassay steps such as by applying microfluidic chip system, use of high end detection system, application of surface modification and protein immobilization strategies to increase the availability of antibodies on the surface, to enhance the antigen-antibody interaction leading to faster analysis and improved sensitivity [52, 53].

Recently, Dixit et al.developed an improved and optimized protocol for rapid and high sensitivity Enzyme Linked Immunoassay (ELISA), by covalently immobilizing antibodies on chemically modified different polymeric substrates [54] . The developed method was rapid and 16 fold more sensitive than already established methods. The aided advantage of the developed protocol was that it could be used for wide range of substrates.

Kuwabara et al. had previously proved that application of nanopillars en-

hances the fluorescence intensity of immunoassay chips. In this work they used nanopillars to increase the surface area for immunoassay [55]. They hypothesized, that the large and controlled surface area of nanopillars increases the amount of biomolecules bound to the chip and enhances fluorescence intensity from markers. They also confirmed the enhancement of fluorescence intensity for the detection of diluted Alfa Feto Protein (AFP) solution.

Apart from using fluorescence microscopy for detection of proteins, Liangcheng et al. also used new plasmonic structure and a self assembled monolayer of molecular spacer to enhance the fluorescence and detection sensitivity for immunoassay of protein A and human immunoglobulin G (IgG) [56]. The average fluorescence increased by over 7400-fold and the immunoassay's detection sensitivity by 3 000 000-fold .

The motivation generated for this research was; firstly, dengue is becoming a major health problem; secondly, no vaccine or treatment is available for curing severe dengue fever; and last but not the least, there is an urgent need of rapid and sensitive diagnostic technique for dengue diagnosis in the early stage of infection.

1.7 Hypothesis

As discussed above, Immunoassay is based upon the principle of Ab-Ag reaction and the Ab-Ag reaction is dependent upon number of factors such as; (a) surface availability of antibodies for the immunoreaction, (b) surface to volume ration and (c) reaction volume. So, we hypothesized that increase in surface area and surface availability of capture antibodies should enhance the sensitivity of Immunoassay for diagnosis of Dengue Virus.

1.8 Objective

To primary objective of this research is to develop sensitive method for diagnosis of Dengue NS1. The research was divided into various sub-objectives to meet the primary objective of the research. The first sub-objective of this the-

sis was to develop an optimized protocol for the preparation of silane monolayer for immobilization of antibodies. The second sub-objective was to characterize the covalently immobilized antibodies on silane monolayer by using different characterization tools such as Fourier Transform Infrared Spectroscopy (FTIR), Ellipsometry, Contact angle measurement, Atomic Force Microscopy (AFM) and Fluorescence microscopy. The third sub-objective of this thesis was to develop a method for diagnosis of dengue NS1 on chemically modified Micro-Spot Integrated Pillars (MSIP) chip .

Optimization and characterization of covalent immobilization of antibodies on silane monolayer has been presented in Chapter 2. A new method for the diagnosis of dengue NS1 has been discussed in Chapter 3. General conclusions as well as future scope of this study has been discussed in Chapter 4.

Chapter 2

Optimization and Characterization of Covalent Immobilization of Antibodies on Silane Monolayer[1]

2.1 Introduction

Immunoassay is a quantitative determination of antigenic substances by serological means and is widely used in various diagnostic tests such as clinical testing and medical diagnostic, pharmaceutical analysis, environmental and food safety testing [52, 57–59]. Solomon Berson and Rosalyn S Yalow discovered the technique in the year 1959 and since then it has found its application for the detection and measurement of a large number of analytes in different solutions [60]. Immunoassay has been conventionally performed on microtiter plate which requires a large volume of samples and reagents. Large volume of samples and reagents lead to longer assay time because of the large diffusion distance required for antibody-antigen reaction [61]. Additionally, there are other disadvantages associated with the conventional immunoassay technique such as, several washing and fluid handling steps, which makes the process tedious and time consuming [52, 57]. Conventional immunoassay also requires established infrastructure of centralized testing facilities to carry out diagnosis

[1] An adaptation of this chapter has been submitted to *Surface Science*, September 2012, *In Review*

of health related diseases. A majority of these disadvantages in conventional methods can be overcome by using microfluidic based immunoassay. Microfluidic based immunoassay requires small volume of samples and reagents, which leads to shorter assay time and makes the whole process less expensive as compared to conventional immunoassay.

Microfluidic based immunoassay has immense potential for simultaneous analysis of several thousands of proteins in biological samples. However, often there are difficulties associated with the immobilization of proteins for such immunoassay [62]. The sensitivity of microfluidic based immunoassay depends on the antibody-antigen reaction, which can be enhanced by increasing the density of immobilized antibodies on the surface [48]. Various protein immobilization methods are available, for example, physical adsorption, covalent, and bioaffinity immobilizations. Among these methods, the covalent immobilization method using self-assembled monolayer (SAM) of organosilane on a silicon surface and SAM of thiol on a gold surface [63] have a great potential and advantages compared to others. Thiol based SAM is formed by the adsorption of an n-alkane thiol on a gold surface whereas SAM of organosilane is obtained by forming siloxane network after reacting with trace amount of water. Silane monolayer generates NH_2 molecules on the surface, which helps in covalently immobilizing the protein with the help of linker molecules such as glutaraldehyde or ethyl (dimethylaminopropyl) carbodiimide (EDC)-N-Hydroxysuccinimide (NHS) [54, 64]. As a result, SAM finds many applications in biosensor development [63, 65]. In the present work, we have optimized the production of silane monolayer on a silicon surface for the immobilization of antibodies.

Typically, silanization process consists of four steps. These are hydrolysis, condensation, hydrogen bond formation and curing [63, 66]. In the first step, hydrolysis of the silicon on interface leads to the formation of the reactive silanol group. In the second step, condensation of these silanol groups takes place leading to the formation of siloxane linkages over the surface. This is followed by oligomerization, forming hydrogen bond with -OH groups on the

substrate. Finally, a covalent bond is formed from silicon of the organosilane on the substrate with the subsequent loss of water molecules. The other two oxygen of APTES molecule either bond to silicon or remain in the free form. This whole process is very sensitive to the presence of water in the system [67, 68]. The silane layer polymerizes in the presence of water to form multilayer of silane [66]. These multilayer are washed away if the silanized surface is kept in any kind of buffer for a long time. The washing of multilayer results in a rough and inhomogeneous surface. Therefore, it is important to perform curing after the incubation step to stop the polymerization of the siloxane layer. Although silanization is a very well-known method of producing a silane layer on silicon surface, it suffers from the demerit that most of the silanization approaches produce a thick and non-uniform silane layer which negatively impacts the sensitivity of any biosensor [69]. There are various other factors that affect the silanization process such as the concentration of the silane, time of incubation, moisture, and temperature of the solution [67, 68, 70].

The SAM is used for immobilizing antibodies on any silicon based inorganic substrate. The immobilization of the antibody is a critical step in the development of highly sensitive microfluidic immunoassay or microchip based assay. For developing a high quality micro immunoassay, it is important that the proteins are immobilized with a high density while maintaining a sufficient distance between each protein molecule. The protein needs to be immobilized in such a manner that the structural integrity and the organization of the protein molecules at the interface are maintained while ensuring that the non-specific adsorption of the proteins is minimal in an order to improve detection performance. The SAM of silane helps in immobilizing the antibodies in a homogeneous manner and the spacer molecule such as glutaraldehyde helps in maintaining sufficient distance between each antibody molecule and reducing the chances of antibodies to touch the substrate surface and hence protect it from denaturation.

Wang and Jin [64] from their study showed that the surface modified with APTES and glutaraldehyde have higher antibody binding capability

compared to Di-chloro dimethylsilane (DDS). They also used mixed silane (APTES+MTES) for covalent immobilization of antibody. The purpose of mixing of silane was to reduce the number of APTES molecule on the surface [71]. Deixit et al. [54] developed an optimized protocol for rapid and high sensitivity Enzyme-linked Immunoassay by covalently immobilizing the antibodies on APTES modified polymeric surface. Libertino et al. [72] used an optimized immobilization protocol to covalently bind the enzyme Glucose oxidase to an oxidized porous silicon surface for monitoring the Glucose oxidase presence on both bulk and porous SiO_2 surface. Ahluwalia et al. [73] studied a number of antibody immobilization techniques for application to optical immunosensors. They focused on the covalent binding and physical adsorption of proteins to improve the density and uniformity in orientation of antibodies on the substrate.

From the existing literature, it is observed that although silanization is a well known process for immobilization of proteins but still an optimized and well characterized protocol for producing silane layer has not been well developed. In the present study, silane monolayer for covalent immobilization of antibodies was prepared. In the experiments conducted, (3-aminopropyl)triethoxy silane (APTES) has been used to prepare monolayer on silicon substrate for protein covalent immobilization. The NH_2 group present at one end of the APTES molecule helps in generating a charged surface and forming a covalent bond with the proteins while the Si-O group at the other end acts as a surface reactive group. Once the monolayer is formed, the surface is treated with glutaraldehyde to yield aldehyde groups on the surface which reacts with the primary amine groups in the exposed lysine residues on the structure of protein to form an amine linkage (see Fig. 2.1).

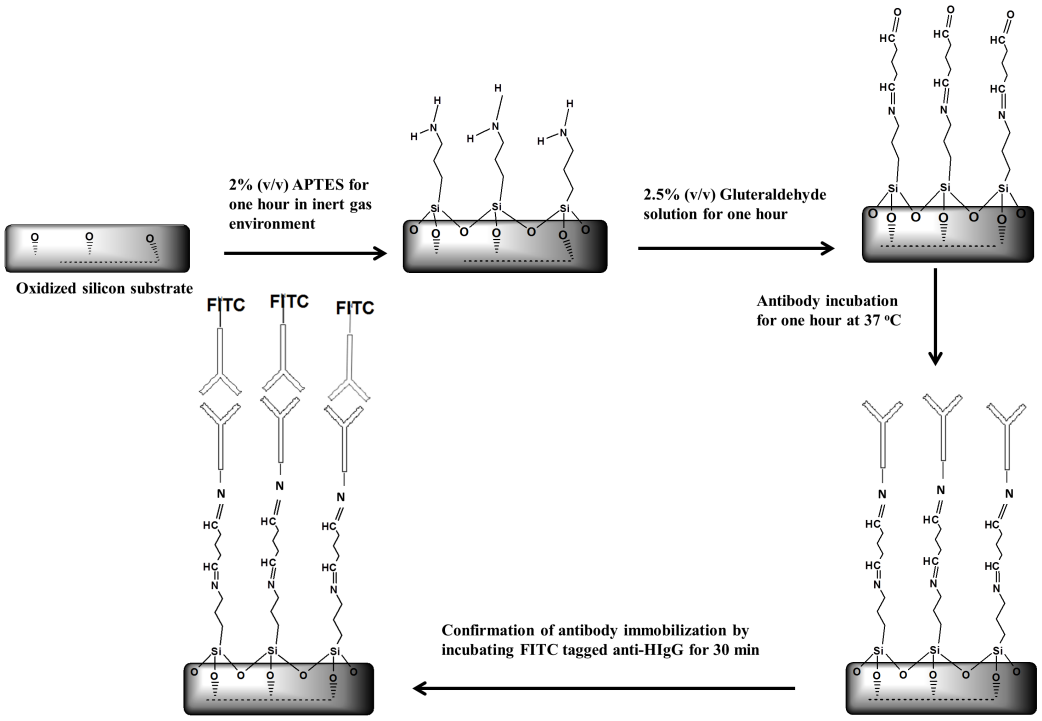

Figure 2.1 – Schematic representation of covalent immobilization of antibodies on silane monolayer. The method involves piranha cleaning and oxygen plasma treatment that generates -O groups on the silicon surfaces, which facilitates the reaction of amine-terminated silane (APTES). The surface is then treated with 2.5% glutaraldehyde to form aldehyde group on the surface that then reacts with the primary amine of the proteins to form an imine linkage. The antibody immobilization was confirmed by using fluorescence microscopy.

2.2 Materials and Methods

2.2.1 Chemicals and Materials

(3-Aminopropyl)triethoxysilane (APTES) and glutaraldehyde (50% aqueous solution) were purchased from Sigma Aldrich, Canada. Human IgG and rabbit secondary human IgG (FITC) were obtained from Abcam, Inc., Cambridge, MA, USA. A 100 mm diameter silicon wafer was bought from Silicon Valley Microelectronics Inc., Santa Clara, CA. The consumable reagents such as toluene (anhydrous, 99.8%), phosphate buffer saline (PBS, pH 7.4), borate buffer and Tween 20 were obtained from Sigma Aldrich.

2.2.2 Characterization Techniques

Spectroscopic Ellipsometry

Spectroscopic Ellipsometry (Sopra GES 5, Semilab USA LLC., Billerica, MA, USA) was used to measure the surface thickness after each step of surface modification and biofunctionalization. All measurements were taken at an incidence angle of 74^o and with the wavelength range of 210 to 920 nm. The data was processed using Winelli Software. The ellipsometric parameters were fitted using dispersion law (Cauchy Law). The experimental and theoretical model best fits were obtained with refractive index of 1.42 and the extinction coefficient (k) set to zero for silane and $k = 0.01$ for glutaraldehyde [74]. For the antibody layer, the best fit was obtained at refractive index of 1.45 and k value equal to zero. Three measurements were taken on each sample to obtain the mean and the standard deviation.

Fourier Transform Infrared Spectroscopy (FTIR)

Thermo Nicolet Nexus (670 FTIR, Thermo Scientific, USA) was used for conducting the chemical analysis of the samples after each step of surface modification. FTIR characterization was carried out at a grazing angle of 75^o. The resolution was 4 cm^{-1} with 1000 scans collected to improve the signal to noise ratio.

Contact Angle Measurement

After each step of surface modification, the contact angle was measured using Kruss DSA 100 (Kruss GmbH, Hamburg, Germany) to observe the change in the surface energy of the silicon surface. The static water contact angle was measured at room temperature using sessile drop method and image analysis of the drop profile. The volume of water used was 5 μL and the contact angle was measured 5 s after the drop was deposited. For each sample the reported value is average of the results obtained for three droplets at three different locations of the substrate.

Atomic Force Microscopy (AFM)

Atomic Force Microscopy (AFM) experiments were carried out with a commercially available Nanoscope III Multimode AFM (Bruker, Santa Barbra, CA). To minimize the force exerted from the scanning tip on the bio-chemically modified silicon surface, the AFM was operated in tapping mode at room temperature. All the measurements were performed in air for higher lateral resolution, using a silicon probe (TESP, Bruker, Santa Barbra, CA) with typical frequency of 300 kHz. The images, having a scan size of 1 $\mu m \times 1\ \mu m$, were collected at a scan rate of 1 Hz with a line resolution of 512 $\times$ 512. All images were flattened using a first order line fit to correct for piezo-derived differences between scan lines using the Nanoscope analysis software provided by Bruker (Santa Barbara, CA). The roughness of the surface was determined by measuring the root-mean-square (RMS) parameter which is defined as the root-mean-square average of the height (z) taken from the mean data plane and can be expressed as $RMS = \sqrt{\frac{1}{N}\sum_{i=1}^{N} {z_i}^2}$, where z_i is the current value and N is the number of points within the analysis section.

Fluorescence Microscopy (FM)

A fully automated bright field and a fluorescence-inverted microscope (Leica DMI6000 B, Leica Microsystems Inc., ON) was used to take the fluorescent

images of the covalently immobilized antibodies on the modified silicon surface. Fluorescence excitation wavelength was in the range of 450 - 490 nm and emission sensitivity was above 520 nm in the experiment.

2.3 Experimental Procedure

2.3.1 Cleaning of Silicon Substrates

Proper cleaning and surface activation of the silicon surface plays a crucial role in the silane growth. For cleaning the silicon substrate, the substrates were kept in a piranha solution (3 : 1 ; H_2SO_4: H_2O_2) for 15 minutes. The substrates were then carefully rinsed with DI water, and dried under a stream of nitrogen gas. The cleaning of the substrate surface removes all the metal and the dust particles that were generated during the dicing step. The piranha solution (strong oxidizing agent) also removes the organic contaminants and makes the surface more hydrophilic by hydroxylating the silicon surface.

After the cleaning step, oxygen plasma treatment at 80 sccm, 150 mT, 225 W RF of the silicon substrate was done to control the activation of the -OH group on the surface, resulting in reducing the surface roughness and improving the formation of homogeneous layer. Plasma treatment controls the hydrophilicity of the surface to improve adhesion for subsequent coating or adsorption of functional groups.

The silicon substrates were then carefully rinsed with DI water and dried under a stream of nitrogen gas. Finally, the substrates were dried in an oven at 110^o C for one hour to remove the moisture present on the surface. It is very critical to dehydrate the surface before the silanization step to avoid the silane bonding reaction with the entrained water molecules and with the surface of the substrate, creating a bond that is actually on the top of hydrated surface.

2.3.2 Preparation of Silane Monolayer

Silane Concentration

For producing a silane monolayer, different concentration of APTES solution was prepared in pre-heated anhydrous toluene (100 - 120^o C). The cleaned silicon substrates were then immersed in a solution of different concentrations of APTES (2%,5%, 10% and 20% and 0.1%, 0.2% and 0.4%) for overnight (time at which the surface has reached saturation for growing silane layer) at room temperature in nitrogen ambient. The silicon substrates were then removed from the solution and rinsed with toluene and 99.5% ethanol and dried in an oven at 100^o C for one hour. All the above steps were carried out in nitrogen glove box to reduce the effect of moisture on the silanization process.

Silanization Time

For producing silane monolayer in minimum amount of time, the cleaned silicon substrates were immersed in a solution of 2% APTES for different time intervals and then left for a night at room temperature in a nitrogen gas environment. The experimental set-up and the conditions remain the same as mentioned earlier.

Experiments were done on a monolayer of silane to characterize every step of surface modification and antibody immobilization on silicon substrate.

2.3.3 Covalent Immobilization of Antibodies on Silane Monolayer

Silanization of Cleaned Silicon using APTES

The cleaning steps were the same as mentioned earlier. The cleaned silicon substrates were then dipped into 2% solution of APTES in anhydrous toluene for 1 h. Anhydrous toluene was pre-heated to 100 - 120^{o}C and added to APTES , the mixture was poured on to the substrate. The silicon substrate was removed from the solution and rinsed with toluene and anhydrous ethanol and dried in an oven at 100^o C for one hour.

Generation of Aldehyde Group using Glutaraldehyde

The APTES modified silicon substrates were washed in PBS and allowed to react with 2.5% v/v glutaraldehyde in PBS for one hour at room temperature, followed by thoroughly rinsing it with DI water to avoid non-specific adsorption of antibody on the silicon substrates.

Human IgG Immobilization

The glutaraldehyde-activated surface was then reacted with 0.1 mg/mL of HIgG in PBS buffer; along with 1% Tween 20 at room temperature for one hour to get a human IgG layer. After this step, 2 mg/mL of bovine serum albumin (BSA) was added to block the remaining surface.

Detection using FITC tagged Anti-Human IgG

In order to confirm the presence of covalently bound antibody on the silicon substrates, the substrates were incubated with FITC tagged anti rabbit HIgG for one hour. The substrates were then rinsed in DI water and dried under a stream of nitrogen gas. Fluorescence images were obtained using fluorescence microscope. Existence of fluorescence confirms the presence of HIgG on the surface.

2.4 Results and Discussion

Several characterization methods have been used for this study. Firstly, FTIR was used to study the chemical attachment of silane to the silicon surface. Secondly, ellipsometer was used to calculate the thickness of each layer on to the surface. Thirdly, contact angle measurement was taken to determine the hydrophobicity and hydrophilicity of the Surface. Fourthly, Atomic Force Microscopy (AFM) was used to observe the surface topography and to calculate the roughness. Lastly, Fluorescence Microscopy was used to confirm the antibody immobilization on the silicon substrate.

2.4.1 Monolayer characterization

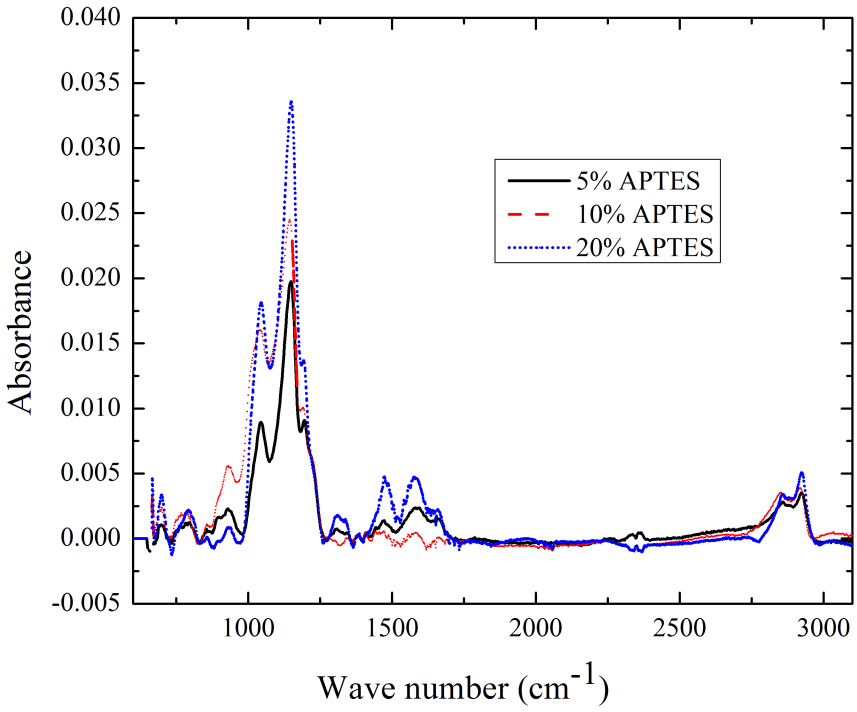

Figure 2.2 – Representative FTIR spectra of APTES chemically attached and referenced to silicon dioxide. The increase in the Si-O-Si band area with increase in silane concentration indicates that more APS is adsorbed at the surface when the concentration of the silane solution is increased.

The amino group (NH_3^+) present at one end of the APTES helps in the conjugation of the protein molecules to the inorganic substrate molecule. The NH_2 group of the APTES molecule generates a charged surface and forms a covalent bond with the proteins with the aid of a linker molecule and the Si-O group at the other end reacts with the silicon surface. Therefore, to achieve an efficient and homogeneous immobilization of the antibodies, it is important that the amino group of the APTES molecule should be oriented away from the surface. The FTIR spectra of the APTES modified silicon surface referenced to the pretreated silicon surface show bands peaking near 1020 - 1140 cm^{-1}.

These bands correspond to a combination of Si-O-Si vibrational bond including those bonds formed between silane and oxide surface, cross linking between silane at the surface and polymerization of silane and unreacted Si-O-C groups. Bands in the region of 2800 cm^{-1} to 2980 cm^{-1} and 1400 to 1700 cm^{-1} are assigned to CH_2 stretching and NH_2 bending, respectively [75, 76]. The Si-O-Si band spectra as shown in Fig. 2.2 increases significantly with increase in the concentration of the silane solution. As the concentration of the silane solution was decreased, the FTIR spectra became very weak because of a very low thickness of the silane layer (> 3 nm) coupled with very low reflectivity of silicon.

In the work presented here, two experimental parameters were explored for silane growth: APTES concentration and silanization time. Thickness of silane layer was measured for different APTES concentration and silanization time using spectroscopic ellipsometer, as shown in Tables 2.1 and 2.2. Table 2.1 shows a gradual increase in the thickness of the silane layer up to a certain concentration (saturation concentration). Since the thickness of the APTES monolayer has been reported approximately as 2 nm, this indicates the presence of multilayer's for higher percentage of APTES solution [74]. Therefore, a thinner silane layer can be obtained by using lower percentage of silane solution. It is also possible to grow a multilayer of silane for lower silane concentration if the silanization time is increased. The thickness of silane layer at a particular concentration for different intervals of time has been shown in Table 2.2. From the Table, it can be deduced that the thickness of silane layer increases with increase in silanization time at a fixed silane concentration (2%). Therefore, it is important to optimize the silane concentration and silanization time to get a thin layer i.e., a monolayer of silane for substrate based bioassays.

Table 2.1 – Spectroscopic Ellipsometry Results: The thickness of the silane layer increases with the increase in concentration.

Concentration of APTES (%)	Thickness of Silane (nm)
0.1	3.2 ±0.1
0.2	3.6 ±0.3
0.4	5.1 ±0.6
2	7.0 ±0.2
5	7.5 ±0.1
10	7.7 ±0.3
20	7.9 ±0.2

Table 2.2 – Spectroscopic Ellipsometry Results: The thickness of the silane layer increases with the increase in silanization time.

Time(h)	Thickness(nm)
1	2.4 ±0.3
2	3.9 ±0.1
4	5.2 ±0.4
12	7.1 ±0.5

2.4.2 Covalent Immobilization of Antibody

FTIR characterization was done after every step of surface modification and antibody immobilization. The spectra obtained were weak (not shown in the paper), which may be due to the low thickness of the layers.

The thickness of different layers formed in the process of surface modification and protein immobilization was measured using spectroscopic ellipsometry, as shown in Fig. 2.3. The thickness of oxide layer was 1.5 ± 0.3 nm. The silane layer thickness was found to be 2.4 ± 0.1 nm, which is close to the reported thickness of silane monolayer (2 nm) [74]. The silanization processes is very sensitive to the presence of water molecule. In the presence of water molecules, the silane layer undergo oligomerization to form multilayer of silane. The thicker layers of silane have a very fragile structure and gets washed away either in the presence of buffer or during various washing steps in an immunoassay process. Hence, it is important to get a monolayer for strong and stable bond formation between silane molecule (NH_2) molecule and antibody. In the present study, a thickness comparable to monolayer of silane was achieved. The

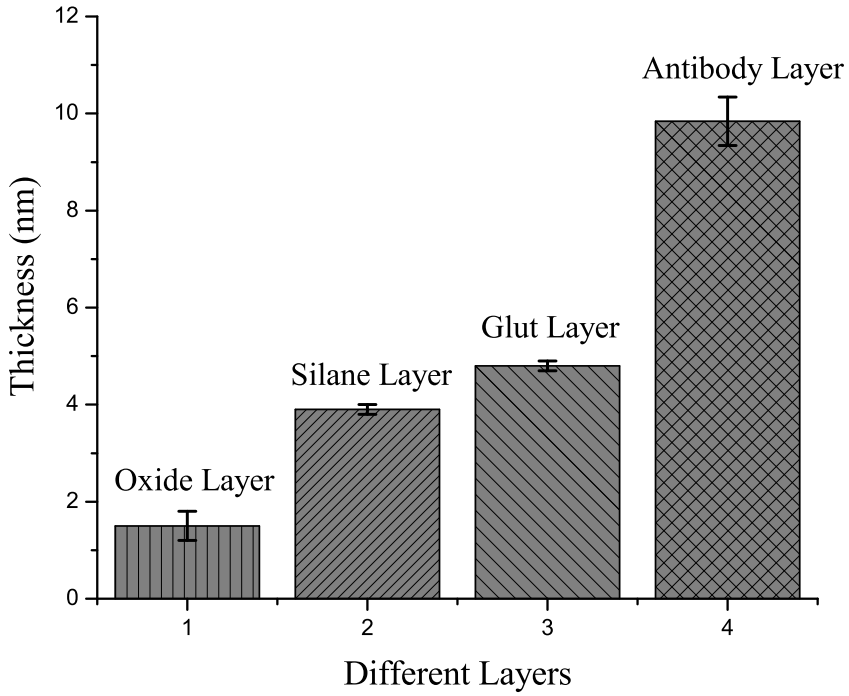

Figure 2.3 – Progressive increase in thickness of different layers after each step of surface modification and protein immobilization.

thickness of glutaraldehyde layer (glut layer) was calculated to be 0.9 ± 0.1nm while the thickness of protein layer was 5.04 ± 0.5nm. The result suggests that there was a gradual increase in the thickness of each layer after every step.

The contact angle of DI water was measured on three different locations of the silicon substrate after each step of the surface modification and bio-functionalization. Before any functionalization, the oxidized silicon surface is found to be more hydrophilic due to the presence of the -OH group. The hydrophobicity is found to be more for silanized silicon surface with water contact angle of $63^o pm 1.5^o$ than for referenced silicon substrate with contact angle of $41^o \pm 0.2^o$. This may be because of the replacement of the -OH group by a more reactive and charged amine group on the surface. After glutaraldehyde treatment the contact angle of the surface was found to be $51.2^o \pm 0.1^o$, which is close to the reported value of contact angle measurement for glutaraldehyde

[77]. This shows that the treatment with glutaraldehyde makes the surface hydrophilic compared to the silanized surface. After the antibody immobilization, the contact angle was found to be $78.2^o \pm 0.5^o$, which can be attributed to the presence of the amine group on the protein structure. This leads to the conclusion that change in contact angle after every step of surface modification and biofunctionalization can be considered as an indicator of change in surface property of the silicon surface.

The surface topography of the chemically modified silicon substrate was studied using AFM. Tapping mode images were acquired following each step of the immobilization process. Figure 2.4 shows the AFM images obtained for the following substrates: (a) a bare silicon surface, (b) a substrate subjected to silanization with APTES, (c) a thin film terminated with glutaraldehyde, and (d) the immobilized antibody (d). A measured RMS roughness of 0.26 nm was observed for the bare silicon substrate (Fig. 2.4(a)). The surface roughness increases considerably with the silanization process resulting in a measured RMS value of 1.74 nm (Fig. 2.4(b)). This increase in roughness can be attributed to the formation of islands of APTES. The chemical ligation of the glutaraldehyde to the amine-terminated surface resulted in a RMS value of 0.35 nm. The result indicates that the glutaraldehyde treatment results in a more homogeneous surface topography as compared to the APTES terminated one. However, an increase in the RMS surface roughness was observed after the antibody immobilization. The RMS surface roughness increased to 0.62 nm which was less compared to the RMS roughness of the silanized surface. The reduction in the surface roughness could be because of the fact that the glutaraldehyde and the antibody treatment might have filled up the cleft and may have smoothened the surface. These values suggest that for all practical purposes, the layers can be considered smooth and the AFM image does indicate a homogeneous interface.

FM was used to investigate the surface coverage and homogeneity of antibody immobilization on the modified silicon. The silanized surface after glutaraldehyde treatment was subjected to antibody (HIgG) immobilization.

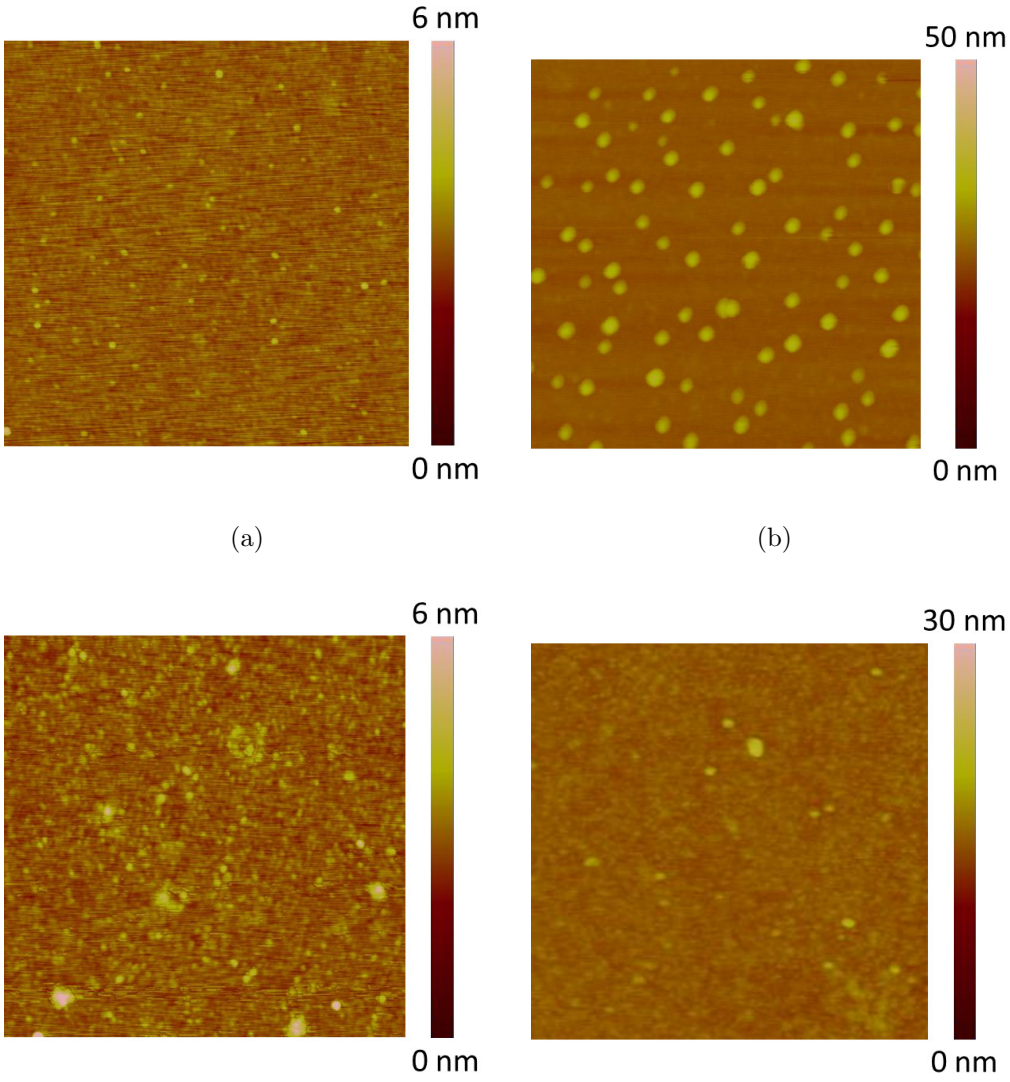

(a) (b)

(c) (d)

Figure 2.4 – 1 mm × 1 mm tapping mode AFM images (a) Cleaned silicon surface, (b) after silanization (c) after Glutaraldehyde treatment and (d) Antibody immobilization.

To confirm the immobilization of the antibody over the modified surface, a 5 μL solution of FITC tagged rabbit anti-HIgG was incubated on it and observed under a FM. Figure 2.5 shows the fluorescence image of FITC tagged anti-HIgG attached to immobilized HIgG on the substrate. It is observed that a uniform fluorescence intensity of FITC-tagged anti-HIgG throughout the surface is obtained in this case. A few high intensity fluorescence spots was observed, which may be due to the agglomeration of antibodies. Figure 2.5 also demonstrates that, the monolayer of silane on a silicon surface is appropriate for immobilization of antibodies for immunoassay.

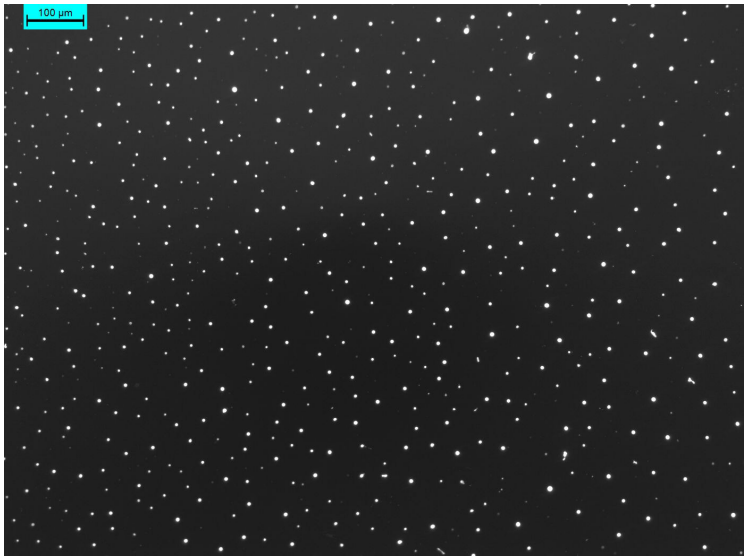

Figure 2.5 – Fluorescence image of FITC tagged anti-HIgG immobilized on silicon surface treated with silanization processes (white spots refer to tagged molecules)

2.5 Conclusion

In this chapter, methods of producing SAM of silane and covalent immobilization of antibodies have been investigated with an objective of increasing the surface density of antibodies for the antibody-antigen reaction. The increase in the antibody-antigen reaction will increase the sensitivity of the immunoassay. In the present work, freshly prepared SAM of APTES on silicon were

chemically investigated using FTIR and the thickness of the layers were calculated using spectroscopic ellipsometer. FTIR spectra suggests the presence of NH_2 group on silicon surface and also confirms the successful deposition of APTES layer. Here we have also reported, a successful procedure for covalent immobilization of proteins on silicon substrates using silane monolayer. The samples were characterized after every step of surface modification and protein immobilization using FTIR, spectroscopic ellipsometer, contact angle measurement system, AFM, and FM. The developed protocol can be used for immobilizing the antibodies for microfluidic or micro-spot based immunoassay, which will lead to rapid diagnosis of multianalytes on the same surface.

The next chapter has shown the application of micropillars for diagnosis of dengue NS1.

Chapter 3

Detection of Dengue NS1 using Micro-Spot with Integrated Pillars (MSIP)[1]

3.1 Background

Immunoassay is a technique that utilizes the highly specific binding between an antigen (analyte) and an antibody to detect or measure the concentration of biologically active compound in different serum or blood samples. Hence, the detection capability of the immunoassay technique depends upon the surface availability and density of the capture antibodies for the immunoreaction. Another important factor that plays a key role in increasing the rate of antibody-antigen (Ab-Ag) reaction, is that the volume of the sample to be tested. As is well known, the time required for reaching equilibrium in substrate-based immunoassay increases in proportion to the ratio of the volume occupied by the solution to that of the volume occupied by reaction interface [61]. Therefore, lesser amount of sample solutions coupled with increased surface area can speed up the immunoreactions. The surface modification and protein immobilization strategies increase the surface density of the immobilized antibodies for the immunoassay that enhances the antigen-antibody interactions leading to faster analysis and improved sensitivity [52, 53]. With the advancement

[1] An adaptation of this chapter has been submitted to *Lab on a Chip*, September 2012, *In review*

of today's technology miniaturized systems such as microfluidic immunoassay, Bio-micro-electro mechanical systems (Bio-MEMS) based on peizoresponse are replacing the conventional techniques because of its inherent advantages such as analysis time, sensitivity and costs.

Baeumner et al. [78] have presented a serotype specific, sensitive and rapid detection of Dengue virus (serotypes 1-4) in blood samples by developing a field-usable RNA biosensor. They used membrane-based DNA/RNA hybridization system in the biosensor for liposome amplification. The capture probes, also known as Dengue serotype specific probes, were immobilized on polyethersulfone membrane strip and reporter probes, also know as generic DNA probe, were coupled to the outside of dye-encapsulating liposomes. The liposomes and the amplified target sequence were mixed and allowed to migrate along the test strip. In their work, the immobilization of the liposome-target complex takes place in the capture zone via hybridization of capture probe with target sequence. The amount of liposome target complex immobilized on capture probe is directly proportional to the target sequence which was further quantified by using reflectometer. Su et al. [79] have also developed an immunochip for the detection of dengue virus. They used Quartz Crystal Microbalance (QCM) as a transducer for detection of dengue virus in aqueous solutions. Two different monoclonal antibodies that act specifically against the dengue virus envelope protein (E-protein) and non-structural 1 protein (NS-1 protein), respectively were immobilized using three different immobilization strategies- Glutaraldehyde, protein A, and carbodiimide method to prepare immunochip. The cocktail immunochip, which has both antibodies attached, was also fabricated and used to compare with the QCM coated with both E-protein and NS-1 protein. An elevation in signal level and increase in sensitivity was observed when both the monoclonal antibodies were immobilized onto the QCM. Zaytseva et al. [80] developed microfluidic based biosensor for rapid, sensitive, and serotype-specific detection of dengue virus using nucleic acid hybridization and fluorescence detection. Zhang et al. [81] investigated the feasibility of dengue virus detection by using silicon nanowire (SiNW)

based sensor for rapid, specific and simple diagnosis of reverse-transcription-polymerase chain reaction (RT-PCR) product of Dengue serotype 2 (DEN-2). In their work, specific peptide nucleic acid (PNA) was covalently attached to the SiNW surface, which was allowed to hybridize with complementary fragment of DEN-2 (69 bp) (obtained from RT-PCR amplification). The change in resistance was measured before and after binding of the RT-PCR product of DEN-2 to the PNA sequence to quantify the dengue virus present in the test sample.

Commercial immunoassay based Enzyme linked immunosorbent assay (ELISA) kits and rapid lateral flow test strips/cassettes are also available for qualitative or semi-quantitative measurement of Dengue NS1 virus concentration in blood serum, plasma and whole blood sample. ELISA kits such as Dengue NS1 antigen and Dengue IgG/IgM ELISA kits are available for detection of dengue infection from different suppliers (for example: Diagnostic Automation, Inc., Calabasas, CA). *In vitro* rapid test strips/cassettes for one step Dengue NS1 Ag test or duo rapid test for Dengue NS1 antigen and IgG or IgM are available commercially from different sources (Standard Diagnostics, Inc., Korea; Biocan Diagnostics, Inc., Vancouver, BC, Canada; Diagnostic Automation and Cortez Diagnstic, Inc., Calabasas, CA). These ELISA and rapid test kits can be used to detect the Dengue antigen or antibody from the blood serum, plasma, or whole blood samples.

However, the current conventional diagnosis methods or the more recently developed microfluidic based methods require complex procedure and technical expertise. Considering the fact that dengue is becoming a global threat and lack of better vaccines or drugs available for dengue infection treatment, it necessitates a need of rapid, sensitive and accurate diagnosis method which can detect dengue in early phase of infection for proper treatment. The aim of the present study is to develop a rapid, sensitive, reliable and accurate diagnosis method for the early detection of dengue virus. In the present work, a rapid and high-sensitivity immunoassay, that utilizes micro-spot with integrated pillars (MSIP), for detection of Dengue non-structural protein (NS1)

has been developed. The method involved fabrication of MSIP; biofunctinalization of the MSIP by covalent immobilization of the Dengue NS1 antibodies; immunoassay on MSIP to detect Dengue NS1 virus; and acquisition of images of MSIP after immunoassay for qualitative and quantitative analysis. An unsupervised, tailor made, probabilistic k-means clustering (PkMC) algorithm was implemented to quantify the fluorescent intensity of acquired images. The effect of diameters, spacing and arrangements of micropillars in MSIP on fluorescent intensity emitted by Dengue NS1 virus was investigated.

3.2 Materials and Methods

3.2.1 Chemicals and Materials

100-mm-diameter silicon (Si) substrate was purchased from Silicon Valley Microelectronics Inc., Santa Clara, CA. 3-Aminopropyltriethoxysilane (APTES), Glutaraldehyde (50% aqueous solution), Toluene (anhydrous, 99.8%), Borate buffer, Phosphate buffer solution and ethanol were purchased from Sigma Aldrich, Canada. Dengue Virus NS1 glycoprotein Protein and Dengue NS1 capture and detection (fluorescein isothiocyanate (FITC) tagged) antibodies were obtained from Faculty of pharmacy and pharmaceutical Sciences, University of Alberta, Canada [82].

3.2.2 Techniques used

Scanning electron microscopy (SEM) and fluorescent microscopy (FM) were used for qualitative and quantitative study of dengue detection. The SEM images of the MSIP were taken before and after immobilization of FITC-tagged Dengue detection antibodies using SEM (LEO 1430, ZEISS, Germany) for qualitative study. FM was used for imaging the MSIPs after immunoassay for both qualitative and quantitative studies using fully automated fluorescence inverted microscope (Leica DMI6000 B, Leica Microsystems Inc., ON) and/or upright microscope (Zeiss Axiostar plus, Carl Zeiss Microscopy, LLC, US).

3.3 Experimental Procedure

3.3.1 Fabrication of MSIP

The Si MSIP were fabricated using the standard microfabrication techniques. Several chips with different configurations, diameters and intervals were designed and fabricated to demonstrate the effect of surface area on enhancement of fluorescent signals. The fabrication procedure of the MSIP is reported elsewhere [83, 84] but briefly described here. A 100-mm-diameter Si substrate was taken and cleaned with Piranha solution. Further, a 0.5-micron thick oxide layer was deposited on top of it followed by patterning of MSIPs on silicon/silicon-dioxide substrate with standard photolithography using HPR506 (Fuji-film Electronic Materials Inc., Mesa, Arizona) positive photoresist (PPR). Subsequently oxide and silicon layers are anisotropically etched in plasma-reactive ion etchers (dry etching technique, DRIE). After etching the silicon for about $\sim 100\ \mu m$, the PPR on the substrate was stripped off using acetone and the substrate was thoroughly cleaned in Branson PPR stripper. Then oxide layer was removed using plasma-reactive ion etchers. Figure 3.1 illustrates the procedure of MSIP fabrication.

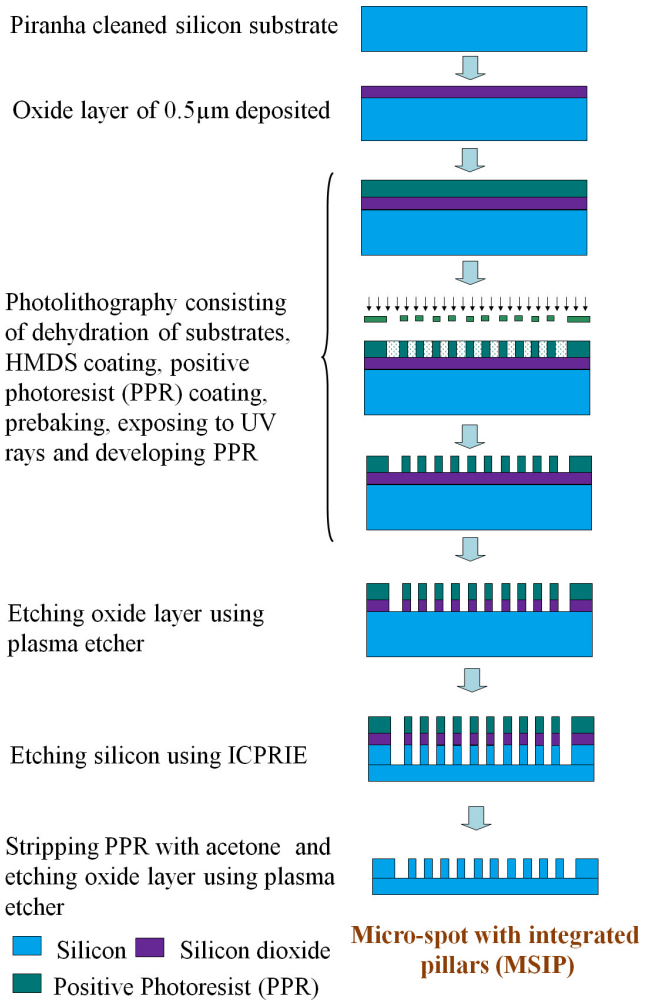

Figure 3.1 – The process flow diagram for the microfabrication of MSIPs

Six different configurations of MSIPs were used for the study. The geometrical parameters of the MSIP are summarized in Table 3.1 and the physical representations of different configurations of MSIP are provided in Fig. 3.2. An SEM image of the micropillars inside the MSIP is shown in Fig. 3.3. Column 1 of Table 3.1 represents the two different spatial arrangements of the pillars, where NSq represents the square arrangement and NSt represents the staggered arrangement. For example, NSq-30-90 corresponds to square arrangement with diameter (d) as 30 μm and distance between two pillars (S) as 90 μm. Column 2, 3 and 4 represents the diameter (d), spacing (S) and height (h) of the micropillars, respectively. The diameters of the micropillars range from 30 to 100 μm; the micropillars spacing/interval ranges from 90 to 135 μm; and the height of the micropillars for all MSIPs is constant and i.e., $\sim$ 98.4 μm. Column 5 represents the total surface area of one pillar. The diameter of the MSIP was 2 mm and the total area of the MSIP was presented in column 6. Column 7 of the Table 3.1 represents the number of pillars present in the MSIP. Detailed equations for calculating these quantities can be found in the Appendix B.

Table 3.1 – Geometrical dimensions of fabricated MSIP

Pillar Arrangement	Diameter d (μm)	Interval $S(\mu m)$	Height $h(\mu m)$	Pillar area $A_{pillar}(\mu m^2)$	MSIP area $A_{spot}(\mu m^2)$	Number of Pillars (n)
NSq-30-84	30	84	98.4	1964	3141600	311
NSt-30-90	30	90	98.4	716	3141600	444
NSq-50-100	50	100	98.4	727	3141600	445
NSt-50-108	50	108	98.4	7853	3141600	199
NSq-100-127	100	127	98.4	7854	3141600	194
NSt-100-135	100	135	98.4	1982	3141600	314

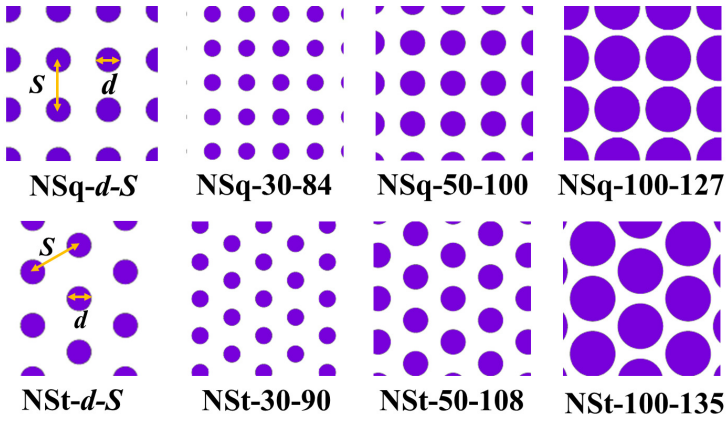

Figure 3.2 – Different configurations of MSIP considered in this work. NSq refers to square arrangement, NSt refers to staggered arrangement, d is the diameter of pillars and S is interval between pillars.

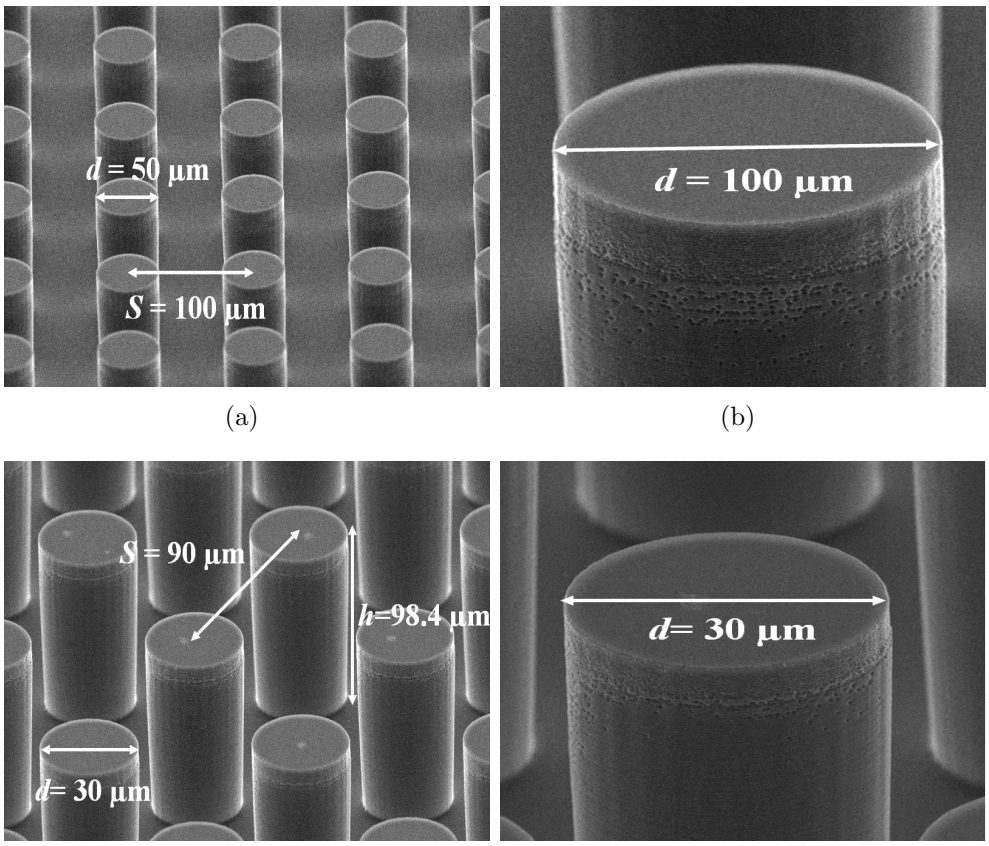

Figure 3.3 – SEM micrograph of the fabricated MSIP. Here, h represents the height of the pillars (98.4 μm, d represents the diameter of pillar, and S represents the distance between two pillars.

3.3.2 Immunoassay of Dengue NS1 detection on MSIP

The immunoassay process developed by Singh et al. [85] for the detection of Dengue NS1 on silicon flat surface using APTES+Glutaraldehyde was performed on these MSIPs. The process of immunoassay includes following steps: (a) Cleaning of MSIP; (b) surface modification (APTES+Glutaraldehyde) for covalent immobilization; (c) biofunctionalization of capture antibodies of Dengue NS1 on MSIP (d) Addition of Dengue NS1 antigens on MSIP; and (e) Detection of Dengue NS1 antigen by adding FITC-tagged Dengue NS1 detection antibodies. Figure 3.4 provides the process flow of immunoassay on MSIP for diagnosis of Dengue NS1. Here a brief procedure of immunoassay is described. Prior to immunoassay, the silicon MSIPs were cleaned in a piranha solution ($3:1 of H_2SO_4:H_2O_2$) for ~ 15 min. Then MSIPs were rinsed with de-ionised (DI) water, and dried under a stream of nitrogen gas. After that, the MSIP was dried in an oven at 110^oC for one hour to remove the moisture present on the surface. A 2% v/v APTES in anhydrous toluene is added to the MSIP and kept for one hour. Anhydrous toluene was pre-heated to $100-120^oC$ before preparing the APTES solution. The whole procedure was conducted in a nitrogen-purged glove box in an inert environment. After modifying MSIP with APTES, MSIPs were rinsed with toluene and ethanol. After that MSIPs were dried in an oven at 100^o C for one hour. The APTES modified silicon MSIPs were washed in borate buffer and allowed to react with 2.5% v/v Glutaraldehyde in borate buffer for one hour at room temperature. Then MSIPs were thoroughly rinsed with Mille-Q deionised (DI) water to avoid non-specific adsorption of antibody. Dengue NS1 capture antibody ($0.01\ mg/ml$) was added to Glutaraldehyde-activated MSIP surface and kept for one hour for reaction. After one hour, the residual aldehyde groups remaining after antibody immobilization were blocked with 2 mg/ml of BSA. The MSIPs were then carefully washed and stored at $+4^o$ C until used. A 5 μl of Dengue NS1 antigen (glycoprotein) aqueous solution was dispensed in MSIP and kept for 30 min. Then, MSIPs were cleaned with PBS. To verify the

binding of Dengue NS1, FITC-tagged Dengue NS1 detection antibody (0.01 mg/ml) was dispensed in MSIP and kept for 60 min at room temperature. Then, MSIPs were cleaned with PBS. A fluorescent microscope was used to capture images of the fluorescent signal from the MSIPs.

3.3.3 Quantification of fluorescent intensity from MSIPs after immunoassay

A fluorescent microscope was used to capture the fluorescent signal from the MSIPs after immunoassay. One of the key challenges in such microfluidic based devices is to accurately quantify the fluorescent intensity from the chip. Recently, Kuwabara et al. [55, 86] had reported the detection of human alpha fetoprotein (AFP) using polystyrene nanopillars. They used FITC tagged antibodies for detection. Microarray scanner was used to take the fluorescent intensity image of the nanopillar chip. The variation of fluorescent intensity from the chip with change in concentration was shown in their results. They haven't reported any quantification of the fluorescent image. To quantify the captured fluorescent images a robust tailor-made image processing method is required because of the variable image quality. The clear advantage of tailor-made method over commercially available image processing method is robustness, sensitivity and less human reliance. Hence, to obtain accurate fluorescent intensity, a custom made image processing methodology was applied for this application. The tailor made algorithm probabilistic k-mean clustering(PkMC) method was applied for automatic, unsupervised and accurate quantification of fluorescence [87]. The image processing algorithm was developed by Purwar et al. on MATLAB 2011b platform to carry out the quantification [87]. Figure 3.5 presents the process flow diagram for segmenting the fluorescent images using PkMC method. Detailed procedure of segmenting the images and quantifying the fluorescent intensity from the images can be found in the supplementary material. Figure 3.6(a) shows the part of the original fluorescent image obtained after the immunoassay on MSIP whereas Fig. 3.6(b) represents the fluorescent cluster of the image overlapping on the

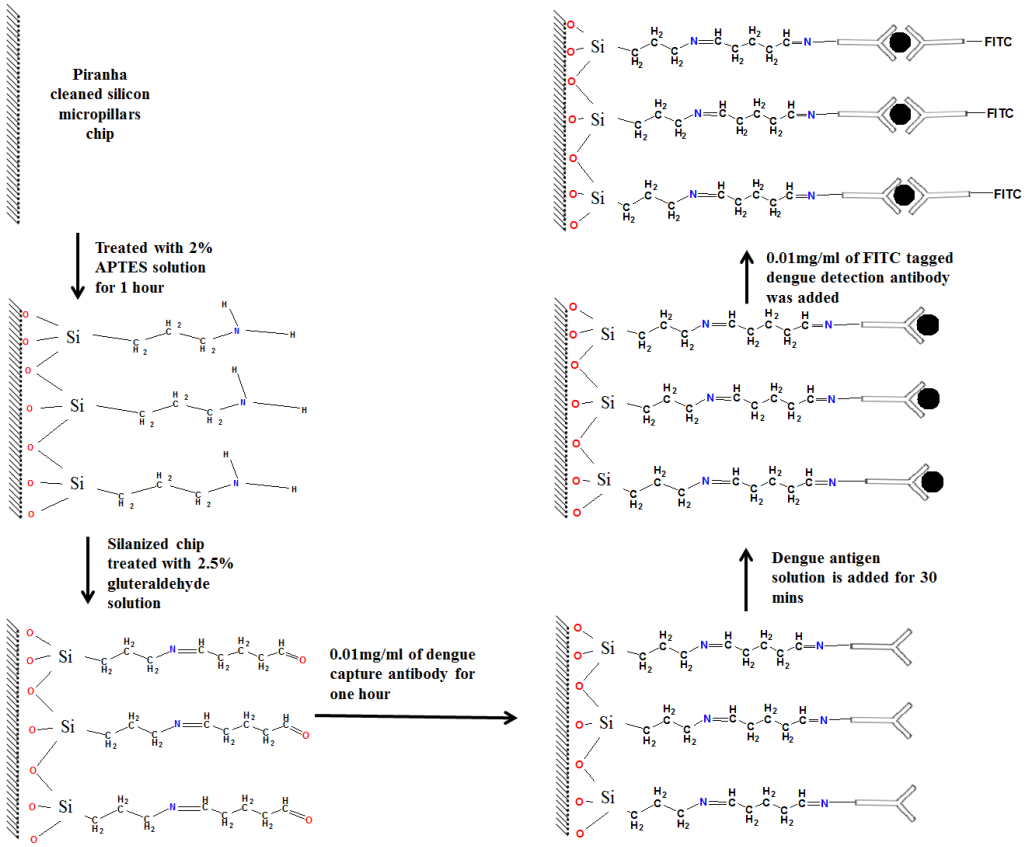

Figure 3.4 – Schematic representation of standard immunoassay procedure on silicon micropillars for detection of Dengue NS1.The method involves: (a) cleaning the silicon micropillars chip with piranha solution, (b) treatment with 2% APTES solution for generating amine group for bioconjugation of antibodies, (c) treatment with 2.5% glutaraldehyde solution for generating aldehyde for forming amide linkage with primary amine of the proteins, (d) addition of Dengue NS1 capture antibodies, (e) addition of different concentrations of Dengue virus antigen solutions and (e) addition of FITC-tagged detection antibodies

original image to clearly show the accuracy of image segmentation used in this work i.e., PkMC method.

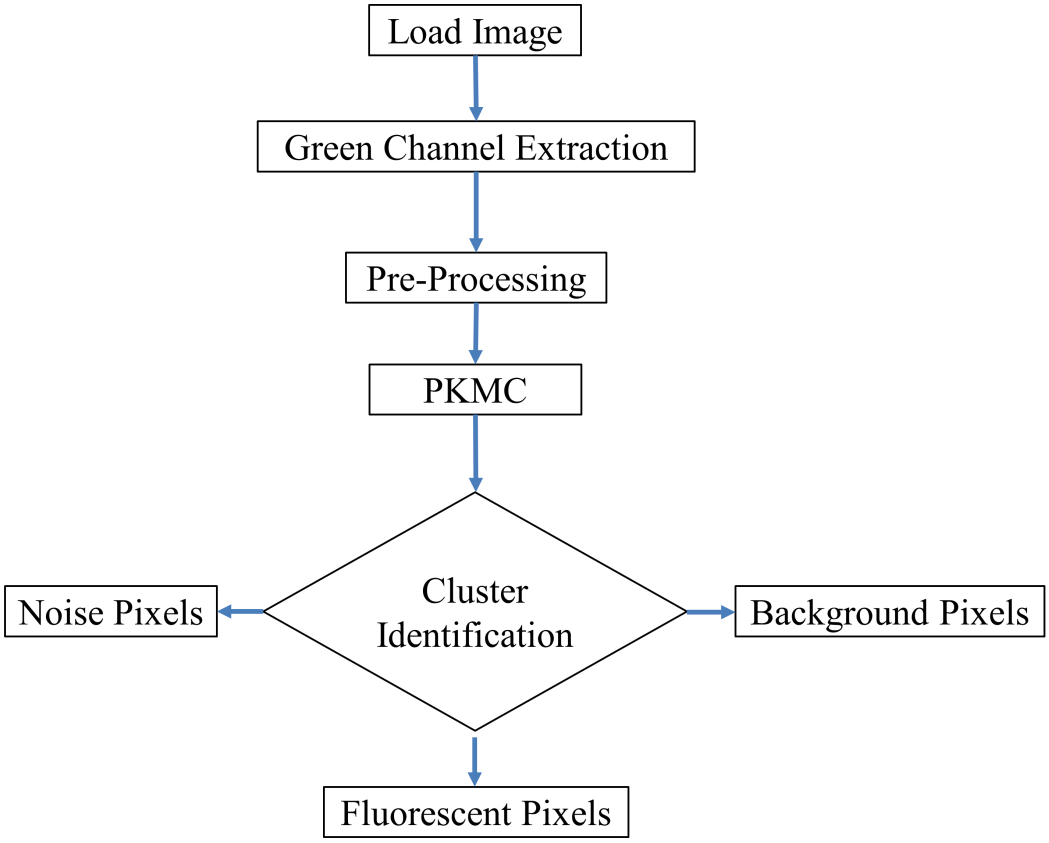

Figure 3.5 – The process flow diagram for segmenting the fluorescent images using PkMC method

3.4 Results and Discussion

The work presented here has demonstrated the combination of qualitative and quantitative analysis of immunoassay performance for Dengue NS1 detection on silicon MSIPs. The sensitivity of immunoassay on different configurations of MSIPs are compared with the flat surface. The schematic representation of immunoassay on MSIP is shown in Fig. 3.7. The insets in Fig. 3.7 depict the distribution pattern of FITC tagged Dengue NS1 detection antibodies on the top of silicon micropillar as well as on the side of the micropillar. Fluorescent

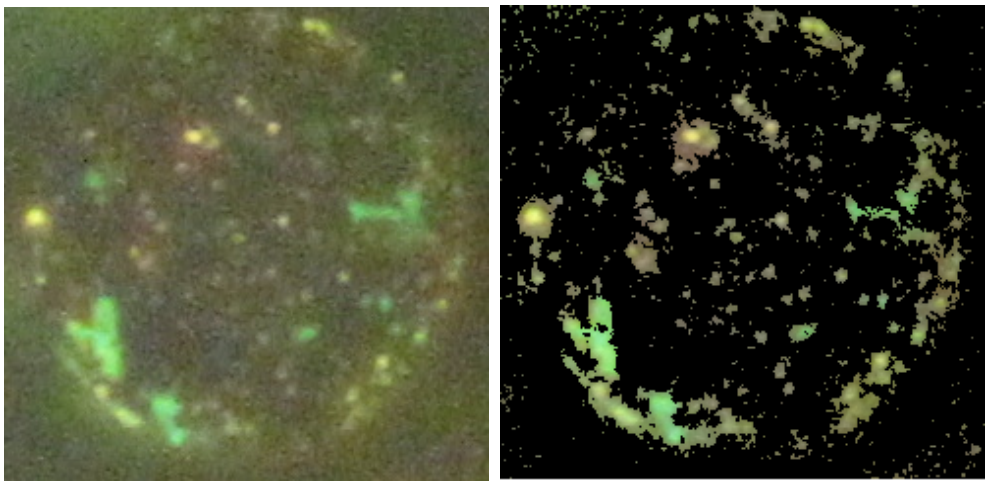

(a) (b)

Figure 3.6 – (a) Part of original captured fluorescent image and (b) processed image after superimposing on original image, to show clear segmentation of fluorescent cluster

microscopy has been used to capture the top view whereas scanning electron microscopy (SEM) has been used to capture the side view of the micropillars after immunoassay. It is observed that the distribution of FITC-tagged Dengue NS1 antibodies has been uniform and homogeneous. These images prove that the surface available for immunoassay is much greater in MSIP because of the availability of the surface for immunoassay on the top, side and between the pillars of the MSIP.

The effect of change in the fluorescence due to the change in concentration of Dengue NS1 antigen was observed using fluorescent microscope and respective fluorescent images were captured for quantification purpose. The acquired fluorescent images were processed using the method developed by Purwar et al. [87] to get intensity values. Detailed procedure of quantifying the fluorescent intensity from the images can be found in the supplementary material. Prior to the quantification of images, the verification test was performed to check the validity of Dengue immunoassay on MSIP using Troponin. A mixture of Troponin ($100ng/ml$) and Dengue NS1 antigens ($100ng/ml$) were

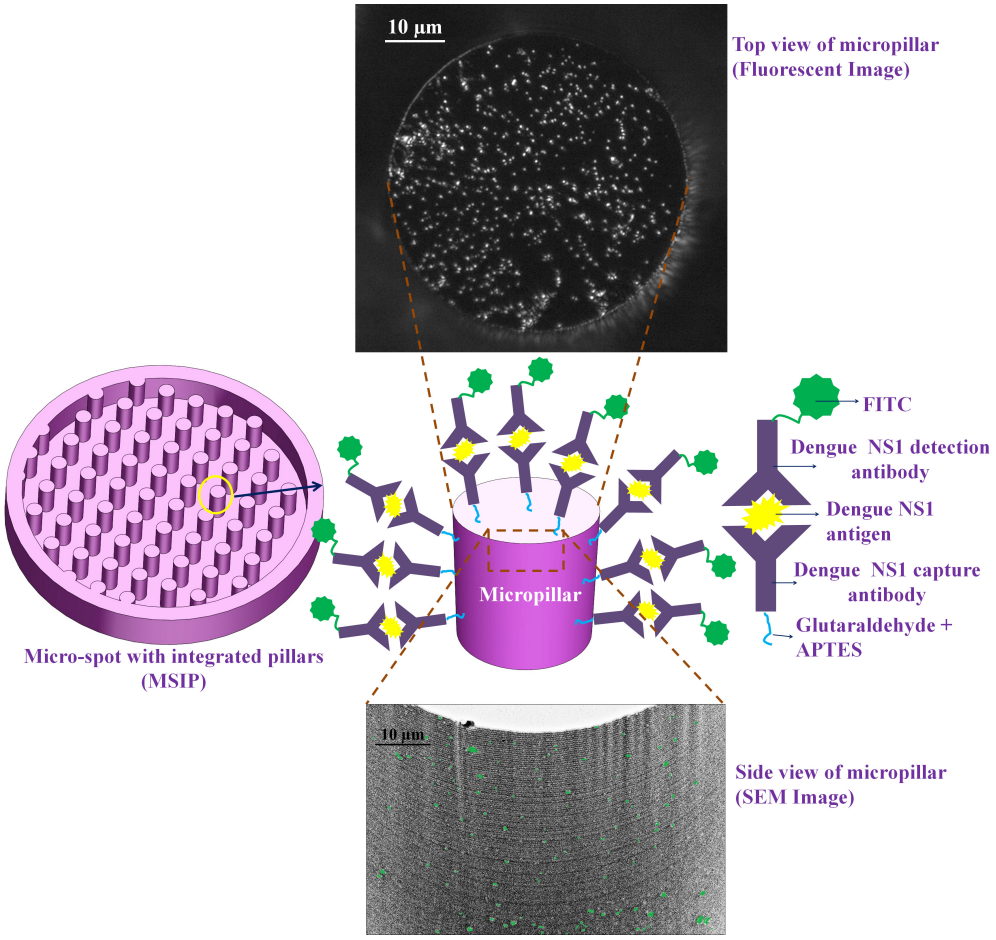

Figure 3.7 – Schematic representation of immunoassay on MSIP (not to scale) with top view (fluorescent image) and side view (SEM image) of one of the micropillars after immunoassay.

added to the MSIP after immobilization of Dengue NS1 capture antibodies. Then, FITC-tagged Dengue NS1 detection antibodies were added to measure the fluorescent signal from the MSIP. It is observed that there is no change in the fluorescent intensity signal of MSIP before and after adding Troponin. This test clearly indicates that the intensities obtained in the present work is totally due to FITC tagged Dengue detection antibodies which are conjugated to Dengue NS1 antigen.

The intensity measurements were repeated three times for each MSIP at each concentration of Dengue NS1 antigen. To determine the uniformity of immunoassay on MSIP, different locations of MSIP for each concentration are processed for error analysis. Details for error estimates can be found in the supplementary material. It is observed that the percentage errors obtained in the fluorescent intensity calculations is $\sim$ 1% or less. Hence the error bars are not shown in the following fluorescent intensity variation plots for different configurations of MSIP. Figure 3.8 depicts the variation of fluorescent intensity of FITC-tagged Dengue NS1 detection antibodies with change in MSIP configuration for different concentration of Dengue NS1 antigens. It is observed that fluorescent intensity decreases with the decrease in surface area. The arrangement of the pillars (staggered or square) does not have any significant difference in terms of the number of pillars actually present in a given MSIP, without substantial change in the total surface area. But, it is found that the fluorescent signal emitted from the staggered arrangement is slightly more compared to square arrangement for the same pillar diameter. This is clearly shown for pillar diamter of 100 μm. It can be concluded that the total intensity of a MSIP depends on the diameter of the pillar, the spacing between the pillars and pillar arrangement.

Experimentally obtained fluorescence intensity values are compared with theoretically estimated intensity values. Figure 3.9 shows the comparison of theoretical estimation of normalized fluorescent intensity of FITC-tagged Dengue NS1 detection antibodies with experimentally obtained intensity values for different configurations of MSIPs. Fluorescent intensity values of dif-

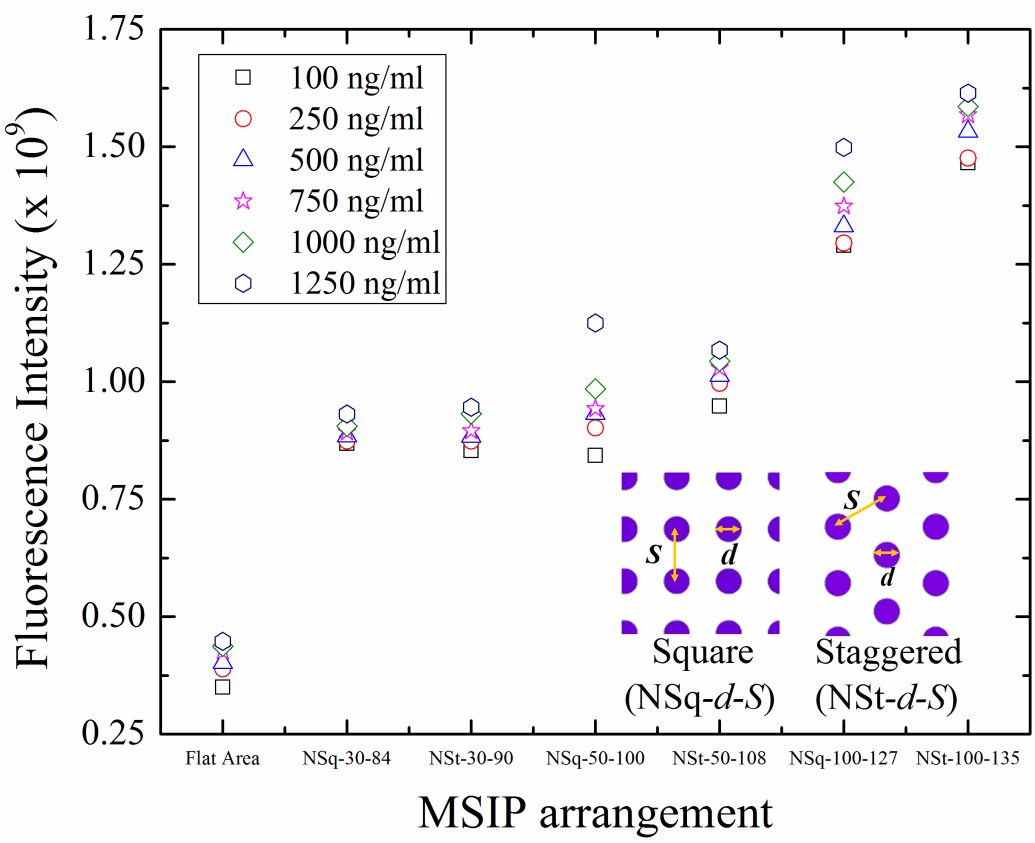

Figure 3.8 – Variation of fluorescent intensity of FITC-tagged Dengue NS1 detection antibodies with change in MSIP configuration for different concentration of Dengue NS1 antigens

ferent configurations of MSIPs are normalized with the fluorescent intensity emitted by flat surface. The theoretical intensity values (see supplementary information for details) shows that the intensity is directly proportional to total surface area of pillars. The plot shows that the experimental intensity values follow the same trend as the theoretically estimated intensity values. Also, experimental values are properly matched with theoretical values for a correction factor of $k = 1.45$. Figure 3.9 illustrates the variation of fluorescent intensity of FITC-tagged Dengue NS1 detection antibodies with change in concentration of Dengue NS1 antigens for different configurations of MSIPs. It is observed that the fluorescent intensity increases with the increase in the concentration of the Dengue NS1 antigen solution. It is also found that the fluorescent signal has significant strength at the lowest concentration of antigen i.e., for 100 ng/ml. This shows that the MSIP can even used for lower concentration of antigen solutions (which is not performed in the present study).

At any particular concentration, the fluorescent intensity value for the flat substrate is significantly less compared to all MSIP configurations. The increased surface area in MSIPs improved the sensitivity of immunoassay compared to the flat surface of the same MSIP size. The increased surface area to volume ratio, reduces the volume of the reagents (or samples) as well as increases the rate of immunoreaction which in turn reduces the incubation time for immunoassay. The arrangement NSt-100-135 shows the highest intensity values for any concentration compared to all other configurations. It is clearly observed that the NSt-100-135 arrangement produces almost 5 folds increase in sensitivity compare to the flat substrate.

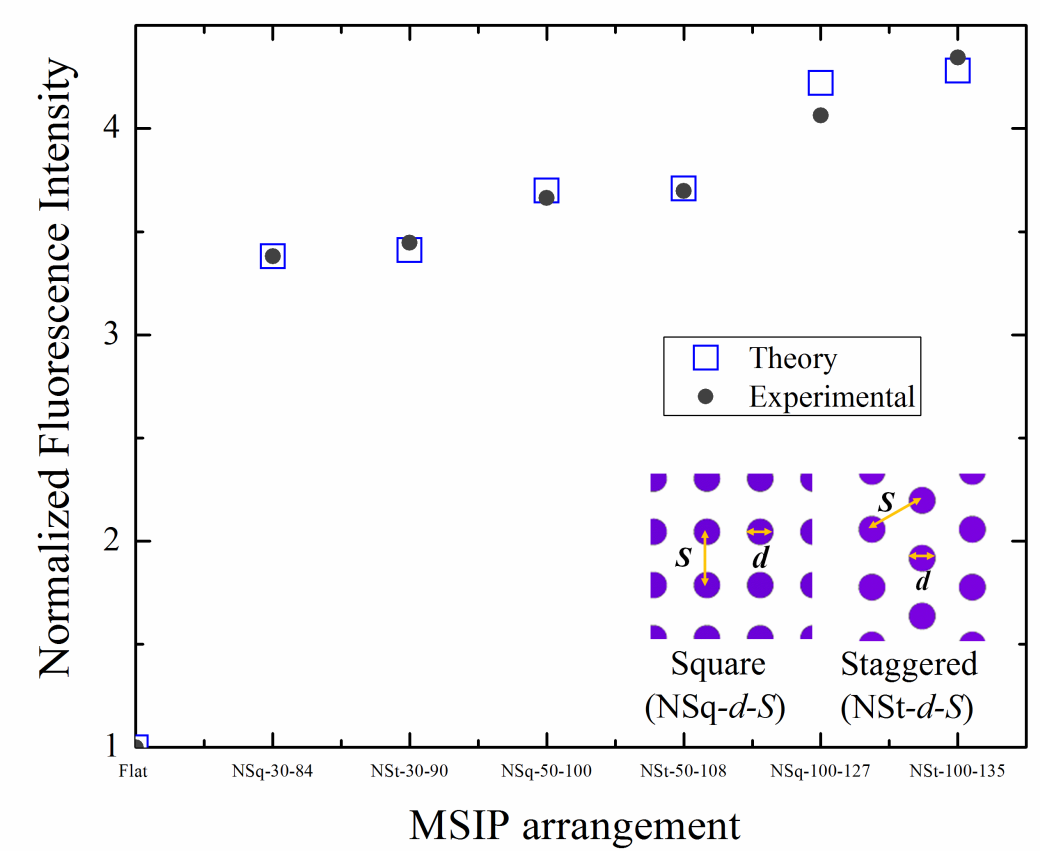

Figure 3.9 – Comparison of theoretical estimation of normalized fluorescent intensity of FITC-tagged Dengue NS1 detection antibodies with experimentally obtained intensity values for different configurations of MSIPs

Figure 3.10 illustrates the variation of fluorescent intensity of FITC-tagged Dengue NS1 detection antibodies with change in concentration of Dengue NS1 antigens for different configurations of MSIPs. It is observed that the fluorescent intensity increases with the increase in the concentration of the Dengue NS1 antigen solution. It is also found that the fluorescent signal has significant strength at the lowest concentration of antigen i.e., for 100 ng/ml. This shows that the MSIP can even used for lower concentration of antigen solutions (which is not performed in the present study). At any particular concentration, the fluorescent intensity value for the flat substrate is significantly less compared to all MSIP configurations. The increased surface area in MSIPs improved the sensitivity of immunoassay compared to the flat surface of the same MSIP size. The increased surface area to volume ratio, reduces the volume of the reagents (or samples) as well as increases the rate of immunoreaction which in turn reduces the incubation time for immunoassay. The arrangement NSt-100-135 shows the highest intensity values for any concentration compared to all other configurations. It is clearly observed that the NSt-100-135 arrangement produces almost 5 folds increase in sensitivity compare to the flat substrate.

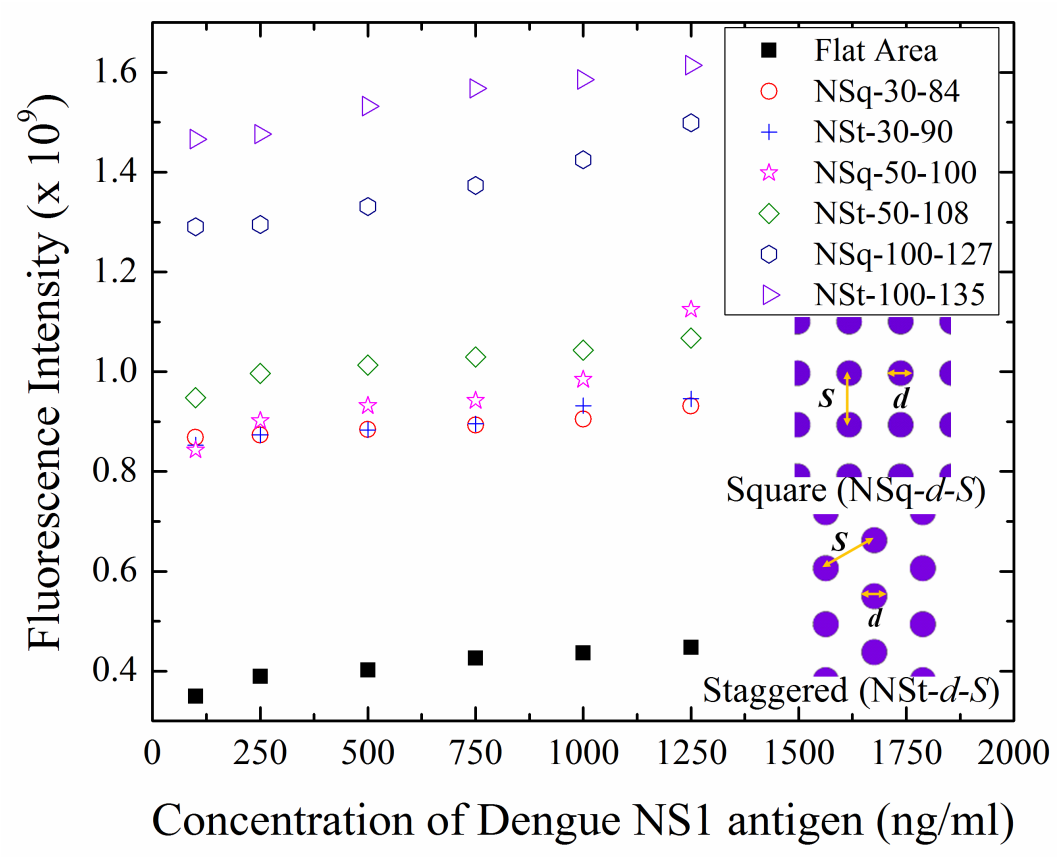

Figure 3.10 – Variation of fluorescent intensity of FITC-tagged Dengue NS1 detection antibodies with change in concentration of Dengue NS1 antigens for different configurations of MSIPs

3.5 Conclusion

In this work, we have developed a new platform, the micro-spot with integrated micropillars (MSIP), for rapid and sensitive detection of Dengue NS1 antigen. Immunoassay for Dengue NS1 was conducted on fabricated MSIPs and captured on fluorescent images for qualitative and quantitative analysis. An automated and unsupervised technique (probabilistic k-mean clustering(PkMC)) was applied to quantify the fluorescence from the captured images. The effect of different diameters, spacing and pillar arrangements in MSIP on fluorescent intensity emitted by MSIP after immunoassay was studied. It is observed that the fluorescent signal emitted from the staggered arrangement is more compared to square arrangement for a same diameter of pillar. It is found that NSt-100-135 arrangement is almost 5 folds more sensitive than the flat substrate. The results obtained in this work can lead to the development of a high throughput detection systems by fabricating multiple MSIP arrays on one chip, which will allow diagnosis of multiple samples simultaneously.

Chapter 4

General discussions, Conclusion and Future works

4.1 General discussions and Conclusion

Miniaturized immunoassay also referred as Lab-on-a-chip, biochip or Micro-Total-Analysis-System is gaining lot of popularity because of many advantages over the conventional detection techniques [52, 57]. Some of the specific advantages associated with the miniaturized immunoassay are: 1) it is faster compared to the conventional technique because of increased surface area to volume ratio, 2) it is relatively less expensive because of lower volumes of samples and reagents requirement and, 3) it has better sensitivity than conventional technique. These advantages potentially improve the overall performance and quality of the assay.

The miniaturized assays can be performed either heterogeneously or homogeneously [52].In heterogeneous immunoassay, the antibodies are immobilized on micro-beads or micro-dimensions chips whereas in homogenous immunoassay, the bound and unbound antibodies are discriminated by applying electric voltage [52]. The performance of heterogeneous immunoassay is greatly dependent on method chosen to bind the antibodies to the surface. The method can either be physiosorption or chemisorption. Chemisorption (covalent attachment), however, is widely used because physiosorption causes the denaturation of proteins which negatively impacts the sensitivity of the assay [64]

.

In this work, a combination of miniaturized immunoassay and covalent immobilization (chemisorption) of antibodies has been used to develop a novel diagnosis method for Dengue fever because of the above-mentioned advantages. The application of the micropillars or nanopillars increases the surface area of the chip than flat surface chips and hence was used in the present work [55]. The increased surface area of the micropillars provides greater surface area for the immobilization of the capture antibodies, which increases the surface density as well as availability of the antibodies for the immunoassay [61]. This leads to increase in rate of immunoreaction, which makes the minitiaurized immunoassay faster compared to conventional immunoassay. The minitiaurized immunoassay also requires very less samples and reagents , which makes it inexpensive method as well [52]. In this work, the capture antibodies were immobilized covalently to reduce the chances of denaturation [64]. The covalent bonding makes the attachment of the proteins to the surface more robust which reduces their chances of getting washed away during the immunoassay, which is major advantage over physiosorption technique.

In order to meet the main objective, which was to develop a novel method for diagnosis of Dengue virus, the research was divided into following steps; development of MSIP chip, conducting immunoassay and finally detection of dengue virus using image based detection method. In our research work, the effect of diameter of the pillars, spacing and arrangement of pillars on fluorescent intensity was investigated however, Kuwabara et.al. have only shown the effect of diameter of nanopillars on fluorescent intensity in their work. In this thesis, chapter 2 describes the preparation of silane monolayer for covalent immobilization of antibodies for immunoassay [86]. Silane concentration and silanization time was optimized for producing silane layer. Silane layer of thickness 2.4nm was successfully produced for the immobilization of capture antibodies. The preparation of silane layer was characterized using ellipsometry and FTIR. The ellipsometer results confirmed the presence of SAM of silane on silicon substrate and the FTIR spectrum showed the presence of NH2 group

in the band area of 1400 to 1700 cm^{-1}. In our research, each step of surface modification and protein immobilization was also characterized by using five different characterization tools (Contact angle measurement system, Fourier Transform Infrared Spectroscopy, Ellipsometry, Atomic Force Microscopy and Fluorescence Microscopy) whereas groups like Wang et.al and other groups have characterized the steps using only one or two characterization tools [64]. The characterization results confirmed that the silicon surface was modified after each step of surface modification and the fluorescence microscopy images confirmed that FITC-tagged antibodies were successfully immobilized on the surface.

In chapter 3, a novel diagnosis method for Dengue non-structural protein (NS1) has been described, which uses synergies of micro-spot with integrated pillars (MSIPs) increased surface area and accuracy of image-based detection. The method involved fabrication of MSIP; biofunctionalization of the MSIP by covalent immobilization of the Dengue NS1 antibodies; immunoassay on MSIP to detect Dengue NS1 virus; and acquisition of images of MSIP after immunoassay for qualitative and quantitative analysis. In our work, we have used image based detection to make the detection process more accurate, robust and unsupervised which is an added advantage of the developed diagnosis technique. Probabilistic k-means clustering (PkMC) algorithm, developed by Purwar et al. [87] was used to quantifying the fluorescent signal from the captured images. This algorithm generates three clusters; 1) background cluster, 2) noise cluster and 3) fluorescent cluster and hence removes the noise and the background from the original image and only provides the quantified value of the fluorescent signals. The commercial available softwares were not used for this work because they have limited ability to process poor quality image and are also incapable of doing segmentation of the images. The qualitative analysis of the captured fluorescent images and the SEM images confirmed the presence of Dengue detection antibodies on the top, side as well as between the pillars. The effect of diameters, spacing and arrangements of micropillars in MSIP on fluorescent intensity emitted was investigated. The quantitative

results confirmed that staggered arrangement of MSIP is more sensitive (gives more intensity signal) than the square arrangement of MSIP for the same concentration of Dengue NS1 antigen. The quantitative results also showed that MSIPs enhances the immunoassay sensitivity, almost 5 times than the flat substrate of the same area. The developed method is relatively simpler and easier to perform when compared to other developed method by different research groups [79–81]. A detailed literature of the existing techniques for the diagnosis of dengue has been provided in chapter 4.

4.2 Limitations and Future work

Silanization is a critical step in the biofunctionalization process but it is complex process and moreover the steps involved in the production of the silane monolayer layer has not been well established and thus, not standardized. Silanization process is dependent upon various factors such as silanization time, silane concentration, pH and moisture. So it is very important to optimize all the parameters for preparing the monolayer of the silane. In the work, the silane concentration and silanization time was optimized but the effect of moisture and pH has not been studied. In future, the effect of moisture and pH on silanization processes can also be studied to get a more optimized condition for producing silane layer.

In this work, MSIP chips were used for detecting dengue virus. This research could be extended to develop a multi-analyte detection system using array of MSIPs on the same chip for diagnosis of different antigens at the same time. This will lead to development of high-throughput detection system which will decrease the total time and cost for the diagnosis of any disease.

In this research work, an algorithm was developed to quantify the fluorescent signals from the captured fluorescent images. Instead of using the fluorescent microscope, confocal microscopy can also be tried to take the images

of the sample for quantitative evaluation. It would enable the reconstruction of three-dimensional structures from the obtained image. The array of MSIP chip can be used to develop a multi analyte detection system for simultaneous diagnosis of different disease at the same time. This approach will reduce the total time and cost for the detection of different diseases.

Real time systems could be developed to diagnose dengue infection on micropillars by capturing fluorescent signals. Image acquisition systems could also be developed to capture real time fluorescent images. This technique will allow more consistent and enhanced quality of images for accurate detection.

References

[1] Fradin M. Mosquitoes and mosquito repellents: a clinician's guide. *Annals of internal medicine*, 128(11):931–940, 1998.

[2] http://www.cdc.gov/dengue/epidemiology/index.html, (accessed July 9, 2012).

[3] Rietveld A and Kouznetsov R. Epidemiology of human malaria plasmodia.

[4] Gardner M, Hall N, Fung E, White O, Berriman M, Hyman R, Carlton J, Pain A, Nelson K, Bowman S, and others . Genome sequence of the human malaria parasite plasmodium falciparum. *Nature*, 419(6906):498–511, 2002.

[5] Phillips R. Current status of malaria and potential for control. *Clinical microbiology reviews*, 14(1):208–226, 2001.

[6] Fact Sheet N. Yellow fever. *TROPICAL DISEASES*, 7(4), 2012.

[7] http://www.who.int/csr/disease/dengue/impact/en/, (accessed July 9, 2012).

[8] MD pgDip tavodovaa M. Dengue fever. *SSMJ*, 5:13, 2007.

[9] Figures F, Capitalization I, Guides A, Dimension A, Translations C, Translations C, Vol F, Translations S, and Vol S. Dengue/dengue hemorrhagic fever: The emergence of a global health problem.

[10] http://www.denguevirusnet.com/history-of-dengue.html, (accessed July 9, 2012).

[11] Pang J, Salim A, Lee V, Hibberd M, Chia K, Leo Y, and Lye D. Diabetes with hypertension as risk factors for adult dengue hemorrhagic fever in a predominantly dengue serotype 2 epidemic: A case control study. *PLoS Neglected Tropical Diseases*, 6(5):e1641, 2012.

[12] Hoek van der W. Human health in water resource development.

[13] Jacobs M. Dengue: emergence as a global public health problem and prospects for control. *Transactions of the Royal Society of Tropical Medicine and Hygiene*, 94(1):7–8, 2000.

[14] Gubler D. Dengue and dengue hemorrhagic fever. *Clinical microbiology reviews*, 11(3):480–496, 1998.

[15] Weaver S. *Frontiers in dengue virus research*. Caister Academic Pr, 2010.

[16] Gubler D. Dengue/dengue haemorrhagic fever: history and current status. *New Treatment Strategies for Dengue and Other Flaviviral Diseases*, pages 3–22, 2006.

[17] Whitehead S, Blaney J, Durbin A, and Murphy B. Prospects for a dengue virus vaccine. *Nature Reviews Microbiology*, 5(7):518–528, 2007.

[18] $http : //microbewiki.kenyon.edu/index.php/dengue_transmission$, (accessed July 9, 2012).

[19] Pepin K and Hanley K. Density-dependent competitive suppression of sylvatic dengue virus by endemic dengue virus in cultured mosquito cells. *Vector-Borne and Zoonotic Diseases*, 8(6):821–828, 2008.

[20] *Dengue: guidelines for diagnosis, treatment, prevention and control*, volume Special Programme for Research and Training in Tropical Diseases and World Health Organization. Department of Control of Neglected

Tropical Diseases and World Health Organization. Epidemic and Pandemic Alert. World Health Organization, 2009.

[21] Gibbons R and Vaughn D. Dengue: an escalating problem. *Bmj*, 324 (7353):1563–1566, 2002.

[22] Sabin A. Research on dengue during world war ii. *The American journal of tropical medicine and hygiene*, 1(1):30–50, 1952.

[23] Waterman S and Gubler D. Dengue fever. *Clinics in dermatology*, 7(1): 117–122, 1989.

[24] Rigau-Pérez J, Clark G, Gubler D, Reiter P, Sanders E, and Vance Vorndam A. Dengue and dengue haemorrhagic fever. *The Lancet*, 352(9132): 971–977, 1998.

[25] Coffey L, Mertens E, Brehin A.-C, Fernandez-Garcia M, Amara A, Desprs P, and Sakuntabhai A. Human genetic determinants of dengue virus susceptibility. *Microbes and Infection*, 11(2):143–156, 2009.

[26] Gubler D, Sather G, and Cunha Fonseca da F. Laboratory diagnosis of dengue and dengue hemorrhagic fever. In *Simposio Internacional sobre Febre Amarela e Dengue*, pages 291–322, 1988.

[27] Guzmán M and Kouri G. Advances in dengue diagnosis. *Clinical and diagnostic laboratory immunology*, 3(6):621, 1996.

[28] Gubler D. Dengue and dengue hemorrhagic fever: its history and resurgence as a global public health problem. *Dengue and dengue hemorrhagic fever*, pages 1–22, 1997.

[29] Peeling R, Artsob H, Pelegrino J, Buchy P, Cardosa M, Devi S, Enria D, Farrar J, Gubler D, Guzman M, and others . Evaluation of diagnostic tests: dengue. *Nature Reviews Microbiology*, 8:S30–S37, 2010.

[30] Hammon W, Rudnick A, Sather G, Rogers K, Morse L, and others . New hemorrhagic fevers of children in the philippines and thailand. *Transactions of the Association of American Physicians*, 73:140, 1960.

[31] Rosen L and Gubler D. The use of mosquitoes to detect and propagate dengue viruses. *The American journal of tropical medicine and hygiene*, 23(6):1153–1160, 1974.

[32] Gubler D, Suharyono W, Sumarmo H, Jahja E, and Saroso J. Virological surveillance for dengue haemorrhagic fever in indonesia using the mosquito inoculation technique. *Bulletin of the World Health Organization*, 57(6):931, 1979.

[33] Kuberski T, Rosen L, and others . A simple technique for the detection of dengue antigen in mosquitoes by immunofluorescence. *The American journal of tropical medicine and hygiene*, 26(3):533, 1977.

[34] Kuno G, Gubler D, Velez M, and Oliver A. Comparative sensitivity of three mosquito cell lines for isolation of dengue viruses. *Bulletin of the World Health Organization*, 63(2):279, 1985.

[35] Igarashi A. Isolation of a singh's aedes albopictus cell clone sensitive to dengue and chikungunya viruses. *Journal of General Virology*, 40(3): 531–544, 1978.

[36] Gubler D, Kuno G, Sather G, Velez M, Oliver A, and others . Mosquito cell cultures and specific monoclonal antibodies in surveillance for dengue viruses. *The American journal of tropical medicine and hygiene*, 33(1): 158, 1984.

[37] Deubel V, Gubler D, and Kuno G. The contribution of molecular techniques to the diagnosis of dengue infection. *New York: CAB International*, pages 335–66, 1997.

[38] Lanciotti R, Calisher C, Gubler D, Chang G, and Vorndam A. Rapid detection and typing of dengue viruses from clinical samples by using reverse

transcriptase-polymerase chain reaction. *Journal of Clinical Microbiology*, 30(3):545–551, 1992.

[39] Clarke D and Casals J. Techniques for hemagglutination and hemagglutination-inhibition with arthropod-borne viruses. *The American journal of tropical medicine and hygiene*, 7(5):561–573, 1958.

[40] Barnes W and Rosen L. Fatal hemorrhagic disease and shock associated with primary dengue infection on a pacific island. *The American journal of tropical medicine and hygiene*, 23(3):495–506, 1974.

[41] Casey H and others . Standardized diagnostic complement fixation method and adaptation to micro test. i. laboratory branch complement fixation method by laboratory branch task force. ii. adaptation of lbcf method to micro technique. *Public health monograph*, 74:1, 1965.

[42] Dulbecco R, Vogt M, Strickland A, and others . A study of the basic aspects of neutralization of two animal viruses, western equine encephalitis virus and poliomyelitis virus. *Virology*, 2(2):162, 1956.

[43] Halstead S. Etiologies of the experimental dengues of siler and simmons. *The American journal of tropical medicine and hygiene*, 23(5):974, 1974.

[44] Kuno G, Gubler D, and Oliver A. *Transactions of the Royal Society of Tropical Medicine and Hygiene*, 87(1):103–105, 1993.

[45] Kuno G, Gomez I, and Gubler D. An elisa procedure for the diagnosis of dengue infections. *Journal of virological methods*, 33(1-2):101–113, 1991.

[46] Lam S, Devi S, Pang T, and others . Detection of specific igm in dengue infection. *The Southeast Asian journal of tropical medicine and public health*, 18(4):532, 1987.

[47] http://www.cdc.gov/dengue/clinicallab/laboratory.html, (accessed July 9, 2012).

[48] Wild D. *The immunoassay handbook*. Elsevier Science, 2005.

[49] Janeway C, Travers P, Walport M, Shlomchik M, and others . The interaction of the antibody molecule with specific antigen. 2001.

[50] Simmons C, Farrar J, Vinh Chau van N, and Wills B. Dengue. *New England Journal of Medicine*, 366(15):1423–1432, 2012.

[51] Guzman M, Halstead S, Artsob H, Buchy P, Farrar J, Gubler D, Hunsperger E, Kroeger A, Margolis H, Martínez E, and others . Dengue: a continuing global threat. *Nature Reviews Microbiology*, 8:S7–S16, 2010.

[52] Ng A, Uddayasankar U, and Wheeler A. Immunoassays in microfluidic systems. *Analytical and bioanalytical chemistry*, 397(3):991–1007, 2010.

[53] Sato K, Mawatari K, and Kitamori T. Microchip-based cell analysis and clinical diagnosis system. *Lab Chip*, 8(12):1992–1998, 2008.

[54] Dixit C, Vashist S, MacCraith B, and O'Kennedy R. Multisubstrate-compatible elisa procedures for rapid and high-sensitivity immunoassays. *Nature Protocols*, 6(4):439–445, 2011.

[55] Kuwabara K, Ogino M, Motowaki S, and Miyauchi A. Fluorescence measurements of nanopillars fabricated by high-aspect-ratio nanoprint technology. *Microelectronic engineering*, 73:752–756, 2004.

[56] Zhou L, Ding F, Chen H, Ding W, Zhang W, and Chou S. Enhancement of immunoassays fluorescence and detection sensitivity using three-dimensional plasmonic nano-antenna-dots array. *Analytical Chemistry-Columbus*, 84(10):4489, 2012.

[57] Lin C, Wang J, Wu H, and Lee G. Microfluidic immunoassays. *Journal of the Association for Laboratory Automation*, 15(3):253–274, 2010.

[58] Baeumner A. Biosensors for environmental pollutants and food contaminants. *Analytical and bioanalytical chemistry*, 377(3):434–445, 2003.

[59] Terry L, White S, and Tigwell L. The application of biosensors to fresh produce and the wider food industry. *Journal of agricultural and food chemistry*, 53(5):1309–1316, 2005.

[60] Twyman R. Immunoassays, applications. 2005.

[61] Butler J. *Immunochemistry of solid-phase immunoassay*. CRC, 1991.

[62] Kusnezow W and Hoheisel J. Solid supports for microarray immunoassays. *Journal of Molecular Recognition*, 16(4):165–176, 2003.

[63] Glass N, Tjeung R, Chan P, Yeo L, and Friend J. Organosilane deposition for microfluidic applications. *Biomicrofluidics*, 5(3):1–7, 2012.

[64] Wang Z and Jin G. Covalent immobilization of proteins for the biosensor based on imaging ellipsometry. *Journal of immunological methods*, 285 (2):237–243, 2004.

[65] Chaki N and Vijayamohanan K. Self-assembled monolayers as a tunable platform for biosensor applications. *Biosensors and Bioelectronics*, 17 (1-2):1–12, 2002.

[66] Arkles B and Dispersants P. Hydrophobicity, hydrophilicity and silanes. *Paint and Coatings Industry magazine*, 2006.

[67] Aissaoui N, Bergaoui L, Landoulsi J, Lambert J, and Boujday S. Silanes layers on silicon surfaces: Mechanism of interaction, stability and influence on protein adsorption. *Langmuir*, 28(1):656–665, 2012.

[68] Krasnoslobodtsev A and Smirnov S. Effect of water on silanization of silica by trimethoxysilanes. *Langmuir*, 18(8):3181–3184, 2002.

[69] Joshi M, Goyal M, Pinto R, and Mukherji S. Characterization of anhydrous silanization and antibody immobilization on silicon dioxide surface. In *Computer Architectures for Machine Perception, 2003 IEEE International Workshop on*, pages 7–11. IEEE.

[70] Lapin N and Chabal Y. Infrared characterization of biotinylated silicon oxide surfaces, surface stability, and specific attachment of streptavidin. *The Journal of Physical Chemistry B*, 113(25):8776–8783, 2009.

[71] Wang Z and Jin G. Silicon surface modification with a mixed¡ i¿ silanes layer¡/i¿ to immobilize proteins for biosensor with imaging ellipsometry. *Colloids and Surfaces B: Biointerfaces*, 34(3):173–177, 2004.

[72] Libertino S, Fichera M, Aiello V, Statello G, Fiorenza P, and Sinatra F. Experimental characterization of proteins immobilized on si-based materials. *Microelectronic engineering*, 84(3):468–473, 2007.

[73] Ahluwalia A, De Rossi D, Ristori C, Schirone A, and Serra G. A comparative study of protein immobilization techniques for optical immunosensors. *Biosensors and Bioelectronics*, 7(3):207–214, 1992.

[74] Nehilla B, Popat K, Vu T, Chowdhury S, Standaert R, Pepperberg D, and Desai T. Neurotransmitter analog tethered to a silicon platform for neurobiomems applications. *Biotechnology and bioengineering*, 87(5):669–674, 2004.

[75] Pasternack R, Rivillon Amy S, and Chabal Y. Attachment of 3-(aminopropyl) triethoxysilane on silicon oxide surfaces: dependence on solution temperature. *Langmuir*, 24(22):12963–12971, 2008.

[76] Socrates G. *Infrared and Raman characteristic group frequencies: tables and charts*. John Wiley & Sons Inc, 2004.

[77] Diao J, Ren D, Engstrom J, and Lee K. A surface modification strategy on silicon nitride for developing biosensors. *Analytical biochemistry*, 343 (2):322–328, 2005.

[78] Baeumner A. J, Schlesinger N. A, Slutzki N. S, Romano J, Lee E. M, and Montagna R. A. Biosensor for dengue virus detection: sensitive, rapid, and serotype specific. *Anal. Chem.*, 74:1442–1448, 2002. doi: 10.1021/ac015675e. URL `http://dx.doi.org/10.1021/ac015675e`.

[79] Su C.-C, Wu T.-Z, Chen L.-K, Yang H.-H, and Tai D.-F. Development of immunochips for the detection of dengue viral antigens. *Analytica Chimica Acta*, 479(2):117–123, 2003. cited By (since 1996) 21.

[80] Zaytseva N. V, Montagna R. A, Lee E. M, and Baeumner A. J. Multi-analyte single-membrane biosensor for the serotype-specific detection of dengue virus. *Anal. Bioanal. Chem.*, 380:46–53, 2004. doi: 10.1007/s00216-004-2724-9. URL `http://dx.doi.org/10.1007/s00216-004-2724-9`.

[81] Zhang G, Zhang L, Huang M, Luo Z, Tay G, Lim E, Kang T, and Chen Y. Silicon nanowire biosensor for highly sensitive and rapid detection of dengue virus. *Sensors and Actuators B: Chemical*, 146(1):138–144, 2010.

[82] Super induction of dengue virus ns1 protein in e. coli. *Protein Expression and Purification*, 66(1):66 – 72, 2009. ISSN 1046-5928.

[83] Gunda N. S. K, Joseph J, Tamayol A, Akbari M, and Mitra S. K. Measurement of pressure drop and flow resistance in microchannels with integrated micropillars. *Microfluidics and Nanofluidics, Submitted*, 2012.

[84] Gunda N. S. K, Bera B, Karadimitriou N, Mitra S. K, and Hassanizadeh S. Reservoir-on-a-chip (roc): A new paradigm in reservoir engineering. *Lab on a Chip - Miniaturisation for Chemistry and Biology*, 11(22):3785–3792, 2011.

[85] Singh M, Gunda N. S. K, Norman L, Kaur K, and Mitra S. K. Optimization and characterization of silane monolayer for covalent immobilization of antibodies. *Applied Surface Science, Submitted*, 2012.

[86] Kuwabara K, Ogino M, Ando T, and Miyauchi A. Enhancement of fluorescence intensity from an immunoassay chip using high-aspect-ratio nanopillars fabricated by nanoimprinting. *Applied Physics Letters*, 93 (3):033904, 2008.

[87] Purwar Y, Shah S. L, Clarke G, Almugairi A, and Muehlenbachs A. Automated and unsupervised detection of malarial parasites in microscopic images. *Malaria Journal*, 10(1):364, 2011.

[88] Rusmini F, Zhong Z, and Feijen J. Protein immobilization strategies for protein biochips. *Biomacromolecules*, 8(6):1775–1789, 2007.

[89] Gonzalez R, Woods R, and Eddins S. *Digital Image Processing Using MATLAB: AND Mathworks, MATLAB Sim SV 07.* Prentice Hall Press, 2007.

Appendix A

Description of Hypothesis

A.1 Chapter 1- Hypothesis

This appendix provides the hypothesis of the present work.

A.1.1 Covalent immobilization of antibodies on silane monolayer

Self assembled monolayer (SAM), of either thiol or alkylsilane on gold or silicon surface respectively, is generally used for bioconjugation of proteins to the inorganic substrate [63]. Application of SAM allows attachment of specific proteins and avoids unspecific binding of other target molecules. Covalent attachment of proteins to SAM, through accessible functional groups of amino acid, constrains the proteins to a fixed position resulting in highly specific binding of proteins to the surface. If the amino acid involved in the binding is not associated with the structure or function of the protein then denaturation of the protein can be avoided [88]. The attachment of proteins to the SAM also allows extensive rinsing, which reduce the chances of non-specific binding of target molecules to the substrate. Therefore, we hypothesize that it is possible to immobilize proteins in oriented manner by covalent attachment of proteins to the SAM, which allows reproducibility, conformational, and structural stability of the capture antibodies for immunoassay. Figure A.1 shows a representative diagram of two different strategies for protein immobilization- (a) Physiosorption of proteins, and (b) Chemisorption of proteins.

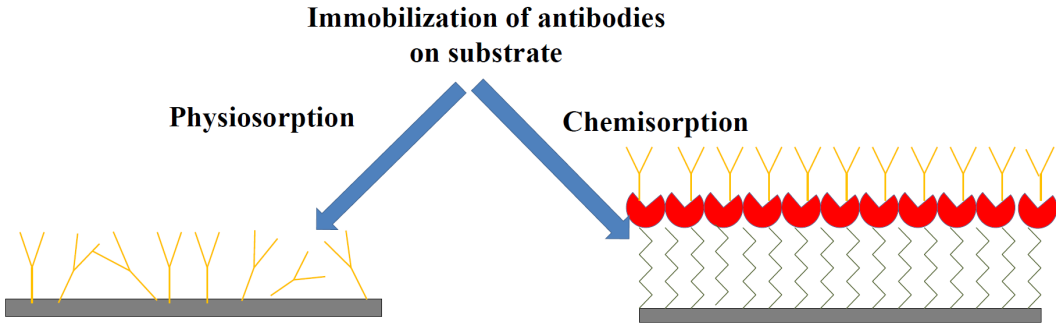

Figure A.1 – Representative diagram showing two different strategies for protein immobilization-(a) Physiosorption of proteins, and (b) Chemisorption of proteins

A.1.2 Enhancement of fluorescent signals using nanopillars and micropillars

Application of micropillars increases the surface area for immunoassay [86]. Hence, we hypothesized that application of high aspect ratio micropillars will increase the surface area for immobilization of capture antibody, which will eventually lead to enhancement of fluorescent signal from FITC-tagged detection antibody. Figure A.2 shows a representative diagram of increase in surface area compared to flat area by using silicon micropillars.

A.1.3 Decrease in sample volume will lead to decrease in diffusion distance

The time required for reaching equilibrium in solid phase or substrate based immunoassay increases in proportion to the ratio of the volume occupied by the sample to that of the volume occupied by reaction interface [61]. Hence, we hypothesized that application of micropillars for immunoassay will increase the surface area and will decrease the diffusion distance which will lead to increase in reaction rate and decrease in incubation time for immunoassay.

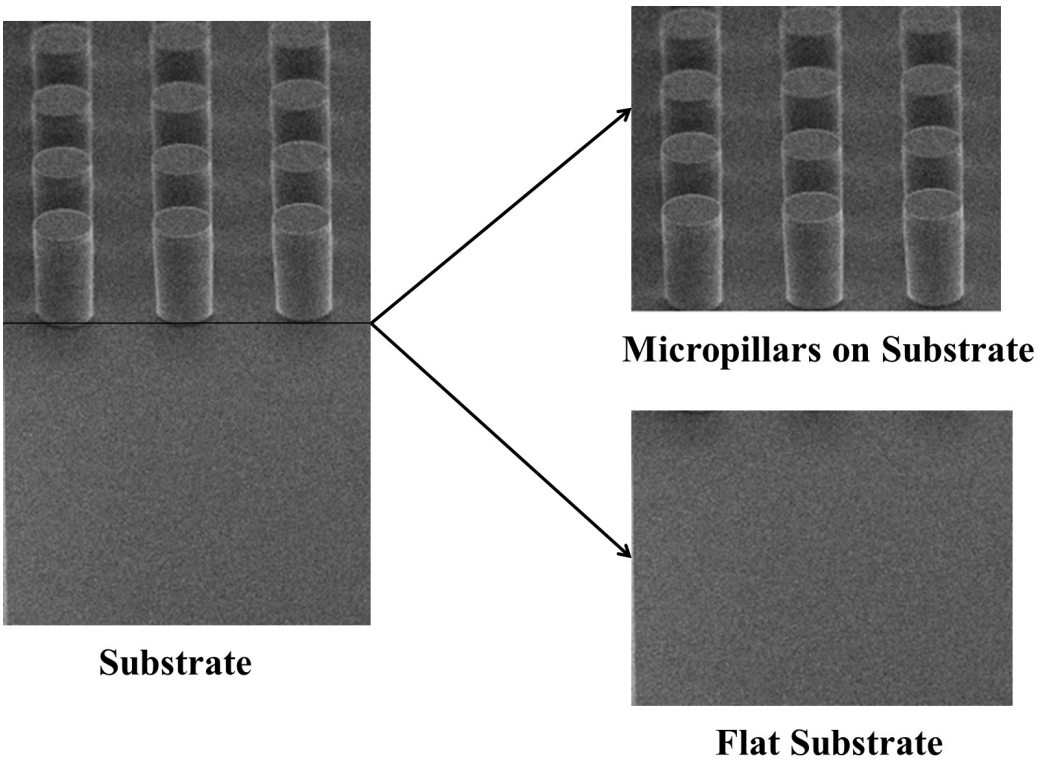

Figure A.2 – Representative diagram showing an increase in surface area compared to flat area by using silicon micropillars

Appendix B

Image Processing Methodology and Error estimates in quantification[1]

B.1 Image Processing Steps

The fluorescent images of the MSIP after immunoassay were processed to quantify the fluorescent intensity. The image processing algorithm developed by Purwar et al. [87] was implemented for these images. Figure B.1 shows the image processing steps for one of the individual pillar to quantify the average fluorescent intensity. The challenge was to achieve high degree of sensitivity and robustness with all the fluorescent images obtained for different configurations of MSIPs, which was carried out using the following steps.

1. Load image: Load original coloured (red, green and blue channel) image obtained from the experiment

2. Green channel extraction: As observed in Fig. B.1(a) the dominant colour is green (due to FITC). Thus, without significant loss of information the green channel or the G image plane was extracted as shown in Fig. B.1(b) from the original colored image for further processing

3. Pre-processing: The purpose of pre-processing is to remove unwanted

[1]This appendix has been included as supplementary material for chapter 3 which is submitted for publication in *Lab Chip*, September 2012, *In review*

noise from the image and to facilitate image segmentation into meaningful regions. The image processing enhances the input image for visual purposes. The contrast of the green channel image was enhanced using local histogram equalization [89] for better visibility of the fluorescent region, as shown in Fig. B.1(c)

4. PkMC *(probabilistic k-means clustering)*: The PkMC technique has been designed by Purwar et al. [87] to capture targeted information within an image. The primary objective in this application is to have a robust and sensitive method for the detection and quantification of fluorescence. In this context, the property of brighter fluorescent pixels can be exploited to separate them from the noise and the background. The visual inspection of pixel intensity data plot, as shown in Fig. B.1(e), reveals distinct clusters of background, noise and fluorescent pixels. The pixel intensity data plot suggests the use of a clustering technique such as k-means clustering (kMC) [89] to segment the pixels into corresponding distinguishable groups. The implementation of robust clustering method requires prior information of a number of clusters and good initial guess of cluster centroids. Commercially available software packages (e.g. MATLAB) provide kMC as a tool for data clustering but these algorithms are not designed for image segmentation. Figure B.1(c) shows that the cluster of fluorescent pixels, presumably has very few data points compared to the noise and the background cluster. Clearly such large data clusters can easily overwhelm the small clusters, with the result that a clear demarcation between the fluorescent pixels is not possible using conventional kMC. To overcome this problem and retaining the information about small clusters in the presence of large clusters, a modified kMC based algorithm has been developed by Purwar et al. [87].

   The small clusters buried alongside large clusters can easily go unnoticed. Therefore the small cluster information would be lost during the process of clustering and hardly any of the small clusters may appear as

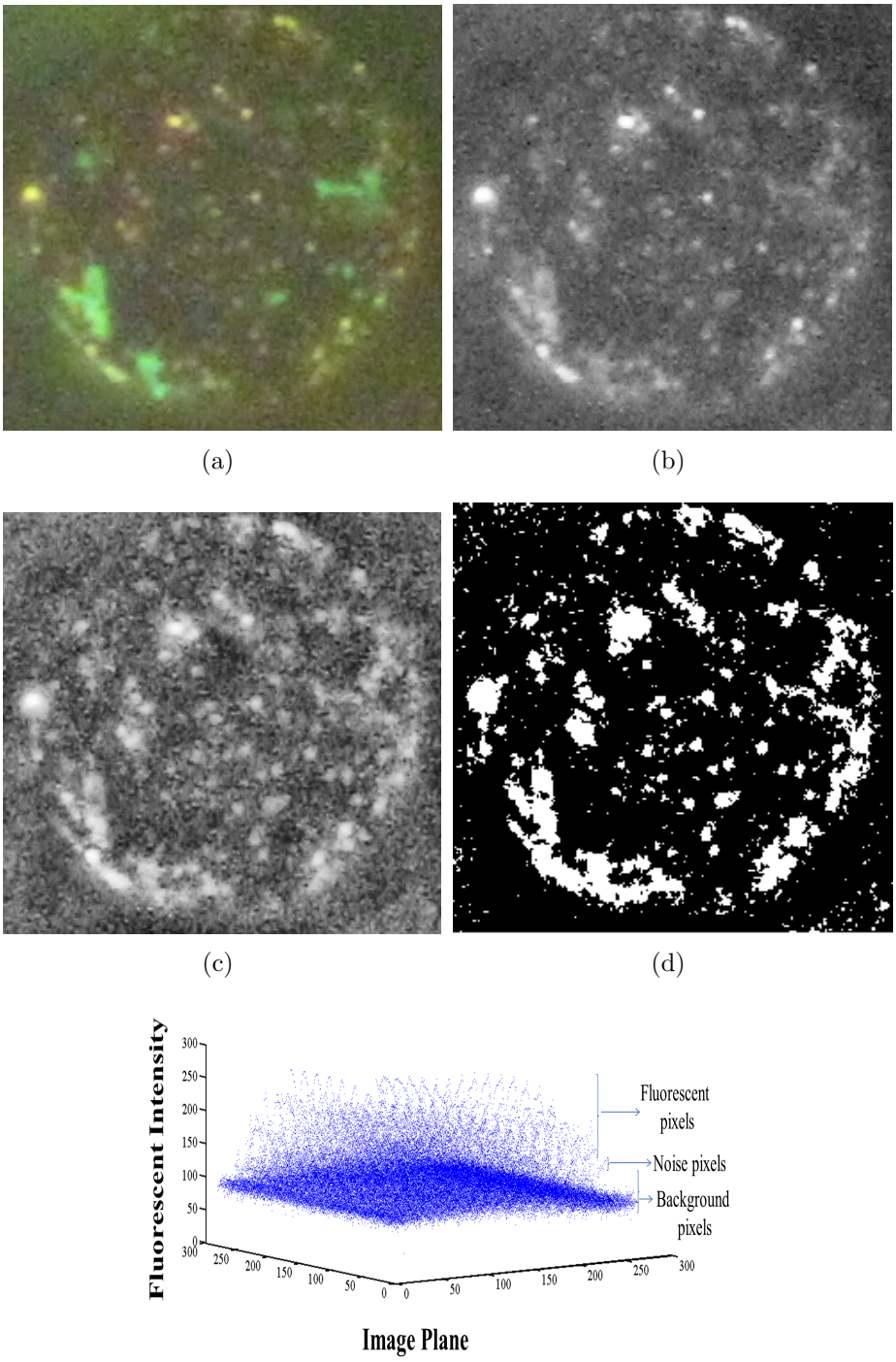

Figure B.1 – Image processing steps; (a) Original image (b) Green channel extracted image (c) Contrast enhanced image (d) Fluorescent pixel image and (e)Pixel intensity plot

separate cluster(s). The solution to this problem is obtained by imparting higher weights to the small cluster(s) compared to the larger clusters. In this way the small cluster information is retained by making the small cluster(s) comparable to big clusters. The new modified form of kMC, as designed with the modifications discussed above, is defined as probabilistic k-means clustering (PkMC). The weights for PkMC are selected using the Binomial theorem. This theorem facilitates the application of dynamic choice of higher weights to small cluster(s).

The PkMC generates three clusters: background, noise and fluorescent pixels as shown in Fig. B.2. Apart from the three clusters the PkMC method also gives the mean intensity of each cluster known as centroids. The third cluster centroid is the quantified mean intensity of the fluorescent pixels. The superimposition of third cluster image i.e., fluorescent pixels on the original image is shown in Fig. B.3, which clearly shows a good segmentation of fluorescent pixels with respect to the remaining image.

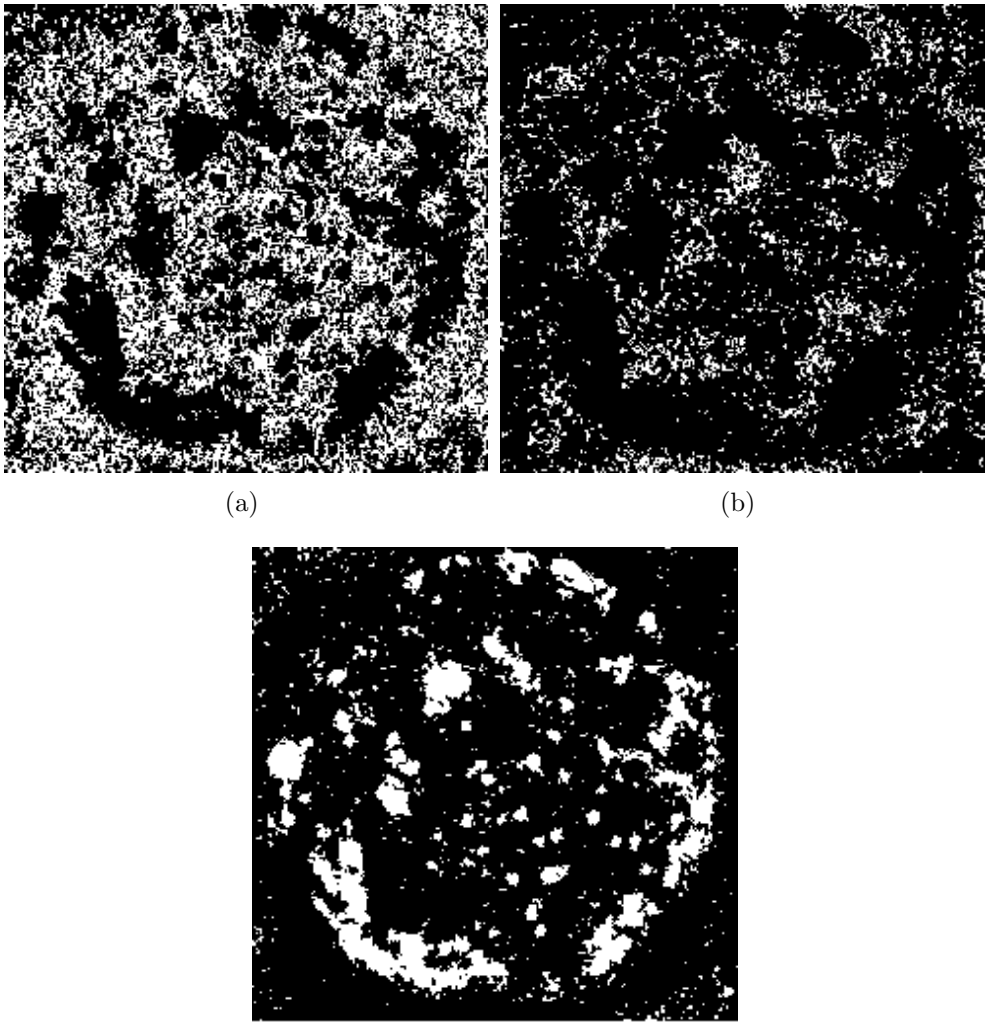

(a) (b)

(c)

Figure B.2 – Image clusters after application of the PkMC algorithm; (a) Background cluster; (b) Noise cluster; (c) Fluorescence cluster

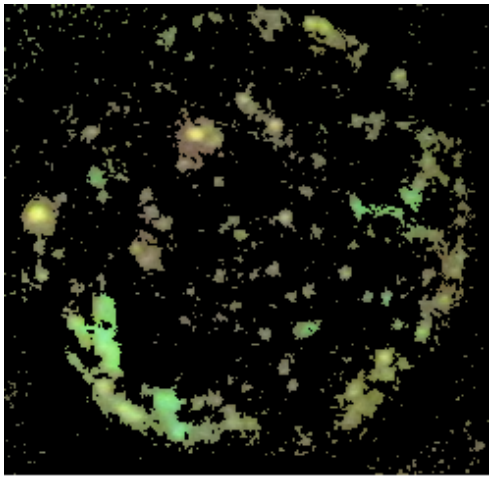

Figure B.3 – Superimposed image of fluorescence cluster shown in Fig. B.2(c) over original image (see Fig. B.1(a))

B.2 Equations used in quantitative analysis

Detailed equations for calculating the total surface area of the pillars, number of pillars and theoretical estimation of fluorescence from the images are provided below.

B.2.1 Total surface area of the pillar

Total surface area of one pillar A_{pillar} is given by:

$$A_{pillar} = \frac{\pi d^2}{4} + \pi dh \tag{B.1}$$

where d is diameter of pillar and h is height of pillar. The first term of Eq. B.1 refers to the surface area of the pillar top ($A_{pillartop}$), whereas the second term of Eq. B.1 refers to lateral surface area of pillar ($A_{pillarlateral}$).

B.2.2 Cross-sectional area of MSIP

The cross-sectional area of MSIP A_{spot} is given by:

$$A_{spot} = \frac{\pi D_{spot}^2}{4} \tag{B.2}$$

where D_{spot} is diameter of MSIP.

B.2.3 Number of pillars

Number of pillars (n) in the micro-spot with integrated pillars (MSIP) can be calculated using the following equation:

$$n = \frac{S_{total}}{A_{pillartop}} \tag{B.3}$$

where S_{total} is total cross-sectional area of MSIP, as given by:

$$S_{total} = \epsilon_s \frac{\pi D_{spot}^2}{4} \tag{B.4}$$

Here ϵ_s is the solid fraction of cross-sectional area of MSIP. The solid fraction (ϵ_s) for different configuration of MSIPs is given as [83]:

$$\epsilon_s = \begin{cases} \frac{\pi d^2}{4S^2} & \text{Square} \\ \frac{\pi d^2}{2\sqrt{3}S^2} & \text{Staggered} \end{cases} \tag{B.5}$$

where S is the interval between two pillars.

B.2.4 Theoretical estimation of fluorescent intensity

The fluorescent intensity I_{th} of MSIP can be calculated theoretically using the following equation [87, 89]:

$$I_{th} = k * I_o * (n * A_{pillarlateral} + A_{spot}) \tag{B.6}$$

where I_o is the fluorescence intensity (obtained from the power of the light source, concentration of antigens, efficiency of the system), k is the correction factor or offset. For the present study $k = 1.45$ is assumed to match the experimental results with theoretical estimated values.

B.3 Error estimates in image intensity quantification

The intensity measurements were repeated three times for each micro-spot with integrated micropillar (MSIP) after immunoassay at each concentration of Dengue NS1 antigen. Usually the errors in quantification of fluorescent intensity from the images can occur due to the difference in thresholding limits. The PkMC technique, which is used in the present study, does not suffer from any type(I or II) of errors due to thresholding since it is robust, accurate and a sensitive method compared to kMC technique(which is used by most of the commercial image processing softwares). To determine the uniformity of immunoassay on MSIP, different locations of MSIP for each concentration are processed for error analysis. Table B.1 provides percentage error in fluorescent intensity calculations for different arrangements of MSIPs at different Dengue NS1 antigen concentrations. It is observed that the percentage errors obtained in the fluorescent intensity calculations is $\sim 1\%$ or less. Hence the error bars for the fluorescent intensity values are not provided in the present work.

Table B.1 – Percentage error in fluorescent intensity calculations for different arrangements of MSIPs at different Dengue NS1 antigen concentrations

Conc. (ng/ml)	Sq-30-84	St-30-90	Sq-50-100	St-50-108	Sq-100-127	St-100-135	Flat Area
100	0.4984	0.4929	0.5284	0.3314	1.0532	0.5632	0.5121
250	0.3822	0.3945	0.1891	0.5383	0.5889	0.4234	0.7506
500	0.4589	0.6937	0.1771	0.4492	0.5048	0.4028	0.4766
750	0.7576	0.8492	0.5779	0.4684	0.7147	0.8858	0.7153
1000	0.5032	0.9169	0.5028	0.4206	0.4875	0.8759	0.4892
1250	0.6392	0.9886	0.5868	0.5584	0.4836	1.0038	0.5123